
THE CAUSAL EFFECTS OF MODIFIED TREATMENT POLICIES UNDER NETWORK INTERFERENCE

Salvador V. Balkus

Department of Biostatistics,
Harvard T.H. Chan School of Public Health
sbalkus@g.harvard.edu

Scott W. Delaney

Department of Environmental Health,
Harvard T.H. Chan School of Public Health
sdelaney@mail.harvard.edu

Nima S. Hejazi

Department of Biostatistics,
Harvard T.H. Chan School of Public Health
nhejazi@hsph.harvard.edu

December 12, 2025

ABSTRACT

Modified treatment policies are a widely applicable class of interventions useful for studying the causal effects of continuous exposures. Approaches to evaluating their causal effects assume no interference, meaning that such effects cannot be learned from data in settings where the exposure of one unit affects the outcomes of others, as is common in spatial or network data. We introduce a new class of intervention-induced modified treatment policies—which we show identify such causal effects in the presence of network interference. Building on recent developments for causal inference in networks, we provide flexible, semi-parametric efficient estimators of the statistical estimand. Numerical experiments demonstrate that an induced modified treatment policy can eliminate the causal, or identification, bias that results from network interference. We use the methodology developed to evaluate the effect of zero-emission vehicle uptake on air pollution in California, strengthening prior evidence.

1 Introduction

Scientists frequently seek to understand the causal effect of a given policy on an outcome Y in a target population. Such policies commonly involve modifying the natural value of some continuous treatment or exposure A ; that is, the value A would have taken had its distribution been left unaltered (Sarvet & Stensrud, 2025). Often, the scientist’s ideal goal is to answer the question, “how would the population mean of Y change if the natural value of A were increased or decreased?”

Modified treatment policies (MTPs) (Robins et al., 2004; Díaz & van der Laan, 2012; Haneuse & Rotnitzky, 2013; Young et al., 2014) are a class of interventions that define causal estimands well-suited for formulating such counterfactual questions about continuous exposures. An MTP can answer the question, “how much would the average value of Y have changed had the natural value of A been increased or decreased by an increment δ ?” where δ is chosen by the investigator. Hence, the MTP provides a *causally interpretable generalization* of the commonly applied procedure of estimating a regression coefficient. In fact, under specific structural assumptions, the effect of applying the MTP $A + 1$ to every study unit is equivalent to the coefficient for the exposure A in a main terms linear regression. Hence, though rarely mentioned explicitly by name, the causal effect of an MTP is a popular target estimand in studies that aim to evaluate policy effects on a well-defined population.

The causal effect of an MTP carries several key advantages over alternative estimands. Unlike the causal dose-response curve, the MTP effect is identified even in settings where it may not be feasible—or, indeed, sensible—to deterministically set each unit’s exposure to the same level. Consequently, the MTP effect is identified even when certain exposure

levels may suffer from non-overlap among sub-populations. Furthermore, the MTP effect estimand admits standard semi-parametric efficient estimators, facilitating the use of machine learning to flexibly capture nonlinear relationships and thus allowing the investigator to mitigate the risks posed by model misspecification.

Like other common causal inference methods, a key assumption of the classical MTP framework is *non-interference*—that one unit’s exposure does not impact any other units’ outcome (Cox, 1958; Rubin, 1980). This critical assumption cannot be made when, for example, study units correspond to geographic areas, such as counties or ZIP code areas. Here, the population units may move around; thus, assigning an exposure policy to a given county would affect not only those residing in that geographic region but also those commuting to and from said region. In general, ignoring interference between units invalidates identification and overtly introduces bias into analytic results (Halloran & Hudgens, 2016). Despite these challenges, data from studies that involve interference between study units can be exceedingly useful, even critical, to advancing science and policy in many settings of current interest. For example, environmental epidemiologists routinely leverage observational spatial data to study the effects of pollution on human health (Elliott & Wartenberg, 2004; Reich et al., 2021; Morrison et al., 2024), a setting in which randomization is impractical and unethical, and where the “shifts in distribution” measured by MTPs are of interest (Tec et al., 2024).

Owing to its straightforward interpretability and the non-restrictive conditions for its identification, especially when compared to other causal estimands for continuous exposures, it is useful to deepen understanding of how to apply the MTP framework even in settings when non-interference cannot be assumed. The present work develops a framework for both identifying and efficiently estimating an MTP’s causal effect under network interference. This allows investigators to obtain inference about the causal effect of a continuous exposure while both accounting for network interference between units and incorporating flexible regression procedures in the estimation process.

Contributions. We present several contributions to the literature on causal inference under network interference. Firstly, we introduce the concept of an *induced MTP*, a new type of intervention that identifies the causal effect of an MTP when network interference is present. This intervention accounts for how the application of an MTP to a given unit affects its neighbors in the known (or assumed) network structure. Secondly, applying the “coarea formula” from measure-theoretic calculus, we provide a novel identification result for the causal effect of an induced MTP in the network setting. Finally, we develop semi-parametric efficient estimators for the causal effect of an induced MTP by applying and building on the prior theoretical contributions of Ogburn et al. (2022). Specifically, we resolve several of their methodological challenges, including (1) using cross-fitted machine learning for nuisance parameter estimation in place of restrictive parametric regression strategies; (2) deriving more tractable forms of the relevant nuisance parameters, which can be reliably estimated using standard regression tools; (3) eliminating reliance on computationally-intensive Monte Carlo procedures for estimation and inference; and (4) obtaining consistent variance estimators.

Outline. Section 2 reviews MTPs and causal inference under interference. Section 3 describes the induced MTP, including identification and estimation of causal effects. Section 4 reports numerical results verifying the proposed methodology, while Section 5 discusses an illustrative data analysis in our motivating applied science context. We conclude and discuss future directions in Section 6.

2 Background

Throughout, we let capital bold letters denote random n -vectors; for instance, $\mathbf{Y} = (Y_1, \dots, Y_n)$. Consider data $\mathbf{O} = (\mathbf{L}, \mathbf{A}, \mathbf{Y}) \sim P \in \mathcal{M}$, where P is the true and unknown data-generating distribution of \mathbf{O} and \mathcal{M} is a non-parametric statistical model (that is, a set of candidate data-generating probability distributions) that places no restrictions on the data-generating distribution. In principle, \mathcal{M} may be restricted to incorporate any available real-world knowledge about the system under study. Let $O_i = (L_i, A_i, Y_i)$ represent measurements on the i^{th} individual data unit, where Y_i is an outcome of interest, A_i is a continuous exposure with support \mathcal{A} , and L_i is a collection of baseline (that is, pre-exposure) covariates. To ease notational burden, we omit subscripts i when referring to an arbitrary unit i (that is, $Y \equiv Y_i$ when the specific unit index is taken to be uninformative).

We will assume that the data-generating process can be expressed via a structural causal model (SCM, Pearl (2000)) encoding the temporal ordering between variables: \mathbf{L} is generated first, then \mathbf{A} , and finally \mathbf{Y} . We denote by $Y(a)$ the counterfactual random variable (or potential outcome) generated by hypothetically intervening upon A to set it to $a \in \mathcal{A}$ and allowing the impact of such an intervention to propagate downstream, to the component of the SCM that generates Y . Our goal is to reason about the causal relationship between \mathbf{A} and \mathbf{Y} in spite of the presence of confounders \mathbf{L} and network interference between units $i = 1, \dots, n$.

2.1 Continuous Exposures with Modified Treatment Policies

A **Modified Treatment Policy** (MTP) is a user-specified function $d(a, l; \delta)$ that maps the observed value a of an exposure A to a new value and may itself depend on the natural (or pre-intervention) value of the exposure (Haneuse & Rotnitzky, 2013).

Example 1 (Additive Shift). For a fixed δ , an *additive shift* MTP may be defined as

$$d(a, l; \delta) = a + \delta. \quad (1)$$

This corresponds to the scientific question, “how much of a change in Y would be caused by adding δ to the observed natural value of a , for all units regardless of their stratum l ?”

Example 2 (Multiplicative Shift). For a fixed δ , a *multiplicative shift* MTP is defined as

$$d(a, l; \delta) = \delta \cdot a. \quad (2)$$

This asks the scientific question, “how much of a change in Y would be caused by scaling the observed natural value of a by δ , for all units regardless of their stratum l ?”

Note that in the above, δ is a fixed, user-specified parameter specifying the magnitude of the hypothetical intervention. However, the MTP framework is even more flexible: interventions that change depending on the values of measured covariates L are allowed.

Example 3 (Piecewise Additive Shift). Consider a piecewise additive function

$$d(a, l; \delta) = \begin{cases} a + \delta \cdot l & a \in \mathcal{A}(l) \\ a & \text{otherwise,} \end{cases} \quad (3)$$

which applies an intervention whose scale depends on the value of a covariate l and only occurs if the natural exposure value a is within some specific subset $\mathcal{A}(l) \subset \mathcal{A}$ of the support of A .

MTPs can be used to define scientifically relevant causal estimands for continuous exposures. The *population intervention causal effect of an MTP* (Díaz & van der Laan, 2012) is defined as $\mathbb{E}_P[Y(d(A, L; \delta)) - Y]$; that is, the average difference between the outcome Y that did occur under the observed natural value of treatment A and the counterfactual outcome $Y(d(A, L; \delta))$ that would have occurred under the investigator-supplied MTP $d(A, L; \delta)$. This estimand answers the scientific question, “what would happen if we applied, to the study population, a policy that modified the existing exposure according to a rule encoded by $d(\cdot; \delta)$?”

When $\delta = 1$, the additive MTP (Example 1) carries the familiar interpretation often attributed to a linear regression coefficient; when $\delta = 1.01$, the multiplicative MTP (Example 2) holds the same interpretation, but for a log-transformed exposure. Hence, MTPs may be seen as a non-parametric and causally interpretable extension of widely used associational estimands, formalizing the problem of quantifying how the mean counterfactual outcome would change under a shift in exposure value. MTPs allow the investigator to specify a wide range of interpretable interventions on continuous exposures that may be carried out in practice. The MTP framework has gained traction for its applicability in settings involving longitudinal, time-varying interventions (Díaz et al., 2023; Hoffman et al., 2024); causal mediation analysis (Díaz & Hejazi, 2020; Hejazi et al., 2023), including with time-varying mediator-confounder feedback (Gilbert et al., 2024); and causal survival analysis under competing risks (Díaz et al., 2024). However, no work has, to our knowledge, extended the MTP framework to settings with dependent data characterized by interference between units.

2.2 Causal Inference Under Interference

Interference occurs when, for a given unit i , the outcome of interest Y_i depends not only on its own assigned exposure A_i but also upon the exposure A_j of at least one other unit ($j \neq i$). Formally, we say interference occurs when $Y(a_i, a_j) \neq Y(a_i, a'_j)$ if $a_j \neq a'_j$. It is a component of the well-known stable unit treatment value assumption (SUTVA; Rubin, 1980), commonly assumed for identification of causal estimands, including those of MTPs (Haneuse & Rotnitzky, 2013; Young et al., 2014).

Previous work has focused on settings exhibiting *partial* interference (Hudgens & Halloran, 2008; Tchetgen Tchetgen & VanderWeele, 2012; Halloran & Hudgens, 2016), which occurs when units can be partitioned into clusters such that interference only occurs between units in the same cluster. Our work focuses instead on a broader setting, that of *network interference* (van der Laan, 2014), which occurs when a unit’s outcome is subject to interference by other units’ exposures according to some arbitrary known network of relationships between units. When such interference

is present, the data \mathbf{O} includes an adjacency matrix or *network profile*, \mathbf{F} , describing each unit's neighboring units, occasionally termed “friends” (Sofrygin & van der Laan, 2017).

Aronow & Samii (2017) demonstrate how to identify a causal estimand when SUTVA is violated due to network interference. To do this, they use an *exposure mapping*: a function that maps the exposure assignment vector \mathbf{A} to the *exposure actually received* by each unit. The exposure received is a function of a unit's original exposure \mathbf{A} and covariates \mathbf{L} , including the network profile \mathbf{F} . If the exposure mapping is correctly specified and consistent, then SUTVA is restored, and causal effects subject to interference can be identified for the exposure arising under the exposure mapping.

Ogburn et al. (2022) and van der Laan (2014) rely on similar logic to identify population causal effects from data exhibiting a causally dependent structure, doing so by constructing “summary functions” of neighboring units' exposures. Notably, they describe semi-parametric theory for efficiently estimating the effects of stochastic interventions in the network dependence setting. Stochastic interventions, which differ from MTPs, replace the natural value of exposure with a random draw from an investigator-supplied counterfactual distribution (Díaz & van der Laan, 2012). While a mathematically elegant strategy, the interpretation of a stochastic intervention is typically challenging—at times, even impractical—as real-world policies can seldom be defined by randomly assigning (post-intervention) exposure values to study units. Furthermore, this setting gives rise to estimation challenges: empirical evaluations in Ogburn et al. (2022) and related work by Sofrygin & van der Laan (2017) relied on relatively bespoke parametric modeling of nuisance parameters, coupled with Monte Carlo procedures for point and variance estimation.

Notably, while the hypothetical exposure that results from this random draw is not guaranteed to match that which would result from an MTP, the two classes of interventions may be constructed to yield equivalent counterfactual means (Young et al., 2014). Given the similarities between these intervention schemes, we extend recent theoretical developments to construct semi-parametric efficient estimators of the effects of MTPs under network interference. Our work reveals that, for MTPs, much of the previously established semi-parametric theory can be reduced in ways that simplify the application of machine learning and adaptive, non-parametric regression for nuisance estimation.

But what does it mean to intervene on a summary function? If one were to intervene on the summary directly, the resulting collection of counterfactual exposures could plausibly be inconsistent with the structure of the network. Some existing works seek to circumvent this issue by recasting the desired estimand as a mean of individual-level causal effects (Aronow & Samii, 2017; Athey et al., 2017; Sävje, 2023). When investigators aim to estimate the impact of a hypothetical policy, however, this strategy will not answer questions of scientific interest—for the estimand does **not** correspond to a population-level intervention that could be implemented in practice. In order to estimate a population-level causal effect, one must consider first intervening, and only *then* applying the summary or exposure mapping—a process more naturally applicable to MTPs.

Other relevant works address interference under different assumptions: random networks (Clark & Handcock, 2024), multiple outcomes (Shin et al., 2023), long-range dependence (Tchetgen Tchetgen et al., 2021; Liu et al., 2025), bipartite graphs (Zigler et al., 2023), and unknown network structure (Ohnishi et al., 2022; Hoshino & Yanagi, 2023). We build on the setting described by Ogburn et al. (2022), as their scientific goals most closely resemble those of the MTP framework.

3 Methodology

Suppose there exists a network describing whether two units are causally dependent with adjacency matrix \mathbf{F} , where F_i denotes the neighbors of unit i . For each unit i , a set of confounders L_i is drawn, followed by an exposure A_i based on a summary L_i^s of its own and its neighbors' confounders, and finally an outcome Y_i based on L_i^s and a summary of its own and its neighbors' exposures, A_i^s . This data-generating process can be defined formally as the SCM in Equation (4):

$$L_i = f_L(\varepsilon_{L_i}); A_i = f_A(L_i^s, \varepsilon_{A_i}); Y_i = f_Y(A_i^s, L_i^s, \varepsilon_{Y_i}). \quad (4)$$

Since A_i^s and L_i^s are not directly observed but are functions that follow from the scientific problem at hand, it follows that (in a slight abuse of notation) $A_i^s = s_{F_i}(\mathbf{A}, \mathbf{L})$ and $L_i^s = s_{F_i}(\mathbf{L})$, which we use to denote that, for unit i , the summary function depends on i 's column of the network adjacency matrix \mathbf{F} . This means that A_i^s and L_i^s depend only on neighboring units. As just one example, A_i^s may be a (possibly weighted) sum of neighbors: $s_{F_i}(\mathbf{A}, \mathbf{L}) = \sum_{j=1}^n F_{ij} A_j = \sum_{F_{ij} \neq 0} A_j$.

Following Ogburn et al. (2022), we assume error vectors $(\varepsilon_{L_1}, \dots, \varepsilon_{L_n})$, $(\varepsilon_{A_1}, \dots, \varepsilon_{A_n})$, and $(\varepsilon_{Y_1}, \dots, \varepsilon_{Y_n})$ are independent of each other, with entries identically distributed and either $\varepsilon_i \perp\!\!\!\perp \varepsilon_j$ provided $\{i, j\} \not\subseteq F_k, \forall k \in 1, \dots, n$ or $\text{Cov}(\varepsilon_i, \varepsilon_j) \geq 0$ otherwise. That is, errors between units are independent provided that the units are neither directly connected nor share ties with a common node in the interference network given by \mathbf{F} ; otherwise, errors across units

may be positively correlated. Positive correlation ensures Theorem 1 will hold, and is typical in applied settings with interference.

Interference bias arises when the data arise from the SCM (4) but investigators wrongly assume that f_Y is a function only of A_i and L_i , and not of $\{A_j : F_{ij} \neq 0\}$ or $\{L_j : F_{ij} \neq 0\}$. Since interference violates the consistency rule (Pearl, 2010), commonly relied upon to identify causal effects, ignoring its presence, even inadvertently, leads to a failure in identification and consequently risks biased estimation. Under the SCM (4), identifiability of the causal effect of applying an exposure to all units $A_j : j \in F_i$ can be restored by controlling for all $L_j : F_{ij} \neq 0$ directly or via the dimension-reducing summaries A_i^s and L_i^s (van der Laan, 2014) of a unit's neighbors' confounders and exposures.

3.1 Induced Modified Treatment Policies

As discussed in Section 2, restoring identifiability by performing inference on A^s and L^s instead of A and L is a common strategy for handling interference. This approach is, however, not compatible with the application of MTPs: one must consider not the causal effect of A under $d(\cdot; \delta)$; but rather, the effect of A^s after intervening on the upstream exposure via $d(\cdot; \delta)$. To identify the causal effects of MTPs under interference, we introduce a novel intervention scheme—the *induced MTP*.

Consider applying an MTP to the SCM (4), replacing \mathbf{A} with the vector $\mathbf{A}^d = d(\mathbf{A}, \mathbf{L}; \delta) = [d(A_i, L_i; \delta)]_{i=1}^n$. Under interference, we are interested in the causal effect of A^s on Y . Hence, the scientific question of interest is actually, “what if A_i^s were replaced by some $A_i^{sod} = s_{F_i}(d(\mathbf{A}, \mathbf{L}; \delta), \mathbf{L})$?” This process is illustrated in Figure 1. We call the function composition $s \circ d$ the *induced MTP*.

$$\mathbf{A} \xrightarrow{d} \mathbf{A}^d \xrightarrow{s} \mathbf{A}^{sod}$$

Figure 1: How an induced MTP arises as the composition of MTP and summary functions $d \circ s_A$.

The counterfactual mean of an induced MTP is given by Equation (5):

$$\Psi_n(\mathbf{P}) = \mathbb{E}_{\mathbf{P}} \left[\frac{1}{n} \sum_{i=1}^n Y(s_{F_i}(d(\mathbf{A}, \mathbf{L}; \delta), \mathbf{L})) \right]. \quad (5)$$

Under an induced MTP, interference no longer hampers identifiability because $s_{F_i}(\mathbf{A}, \mathbf{L})$ captures the contribution of all relevant units (that is, a given unit i and its neighbors) to each Y_i . This data-adaptive parameter will converge to the population counterfactual mean as $n \rightarrow \infty$ (Hubbard et al., 2016). Use of such a parameter definition is necessary because we must condition on the single observation of the interference network at play. Hence, do note that in all theory that follows, our estimates will implicitly condition on the observed network \mathbf{F} . This estimand must be compatible with the network: it is interpreted as the average change in Y caused by imposing the unit-level MTP d on each unit in the population governed by the network \mathbf{F} . With $\Psi_n(\mathbf{P})$ identified, the population intervention effect (a contrast) may be defined by subtracting $\mathbb{E}Y$ (Díaz & van der Laan, 2012).

3.2 Identification

In addition to the SCM (4), to identify the causal parameter $\Psi_n(\mathbf{P})$ by a statistical parameter ψ_n , we rely on the following assumptions:

A1 (Summary positivity). If the summaries satisfy $(s_{F_i}(\mathbf{a}, \mathbf{l}), s_{F_i}(\mathbf{l})) \in \text{supp}\{A_i^s, L_i^s\}$, then the summaries after intervention satisfy $(s_{F_i}(\mathbf{a}^d, \mathbf{l}), s_{F_i}(\mathbf{l})) \in \text{supp}\{A_i^s, L_i^s\}$.

Assumption A1 is a weaker positivity requirement than that required for identification of the causal dose-response curve—rather than requiring all possible exposure values to be observable for every combination of covariates, we only require that the MTP keep the exposure of each unit within the support defined by its *own* covariates, that is, for its own stratum. To some extent, this can be enforced by design if the investigator were to choose d appropriately. Furthermore, Assumption A1 is even weaker than the standard MTP positivity assumption: technically, $A_j^d \in \text{supp}\{A, L\}$ for all $j \in F_i$ is not required, only that the summary A_i^{sod} remains in the support of A_i^s . In other words, we do not require positivity for individual exposures, *only positivity on the summary as a whole*. Importantly, $\text{supp}\{A_i^s, L_i^s\}$ denotes the support of A_i^s and L_i^s together implied by the number of neighbors F_i , as, under a fixed network adjacency matrix \mathbf{F} , the summary function that produces A_i^s may depend on \mathbf{L} and F_i . Since $\text{supp}\{A_i^s, L_i^s\}$ may differ for each unit depending on the number of neighbors, this could be much smaller than $A_i^s \otimes \mathcal{L}_i^s$ for certain summaries.

A2 (No unmeasured confounding). The potential outcome satisfies the condition $Y(s_{F_i}(\mathbf{a}, \mathbf{L})) \perp\!\!\!\perp s_{F_i}(\mathbf{A}, \mathbf{L}) \mid \mathbf{L}$ for all $\mathbf{a} \in \mathcal{A}^n$ and $i \in \{1, \dots, n\}$.

This assumption may be interpreted as slightly weaker than the typical no unmeasured confounding assumption in causal inference: we only require that potential outcomes of a unit i are independent of all possible exposure summaries that could be obtained conditional on the neighbors involved in the summary. For example, if a particular unit's summary only depends on a single neighbor's exposure, then for that unit, the analysis need only adjust for its neighbor's confounders in addition to its own.

A3 (Piecewise smooth invertibility). The MTP $d(a, l; \delta)$ has an inverse defined

$$d^{-1}(a, l; \delta) = \sum_{k=1}^{K(l)} h_k(a, l; \delta) \mathbb{I}(a \in \mathcal{A}_k(l)), \quad (6)$$

for some countable set of functions $h_1, \dots, h_{K(l)}$, where each h_k is continuously differentiable with respect to a over the partition $\mathcal{A}_k(l)$, a set which may depend on the covariates l .

Assumption A3 was first introduced by Haneuse & Rotnitzky (2013) and is standard in the MTP literature (Díaz & van der Laan, 2018; Hejazi et al., 2022; Díaz et al., 2023), where it has been used to ensure the existence of the efficient influence function, allowing for the construction of regular asymptotically linear estimators of the corresponding statistical estimand.

A4 (Summary coarea). The *coarea* of $s_{F_i}(\mathbf{a}, \mathbf{l})$ exists and exceeds zero almost everywhere. That is, for almost all \mathbf{a} , s_{F_i} has a Jacobian $J_{\mathbf{a}}$ with respect to \mathbf{a} satisfying

$$\sqrt{\det J_{\mathbf{a}} s_{F_i}(\mathbf{a}, \mathbf{l}) J_{\mathbf{a}} s_{F_i}(\mathbf{a}, \mathbf{l})^\top} > 0. \quad (7)$$

In Equation 7, the left-hand side is called the coarea of s . See Negro (2022) for a discussion of coarea in statistics. Together, Assumptions A3 and A4 ensure that the causal estimand can be expressed as an estimable function of A_i^s and L_i^s instead of the entire vectors \mathbf{A} and \mathbf{L} , and that its efficient influence function exists, which permits the construction of regular asymptotically linear estimators capable of achieving the semi-parametric efficiency bound.

Under Assumptions A1–A4, the counterfactual mean of an induced MTP $\Psi_n(\mathbf{P})$ is identified by

$$\psi_n = \frac{1}{n} \sum_{i=1}^n \mathbb{E}_{\mathbf{P}}(m(A_i^s, L_i^s) \cdot r(A_i^s, A_i^{s \circ d}, L_i^s) \cdot w(\mathbf{A}, \mathbf{L}, i)), \quad (8)$$

where, letting $J_{\mathbf{a}}$ denote the Jacobian with respect to \mathbf{a} , the nuisances m , r , and w are defined:

$$m(a^s, l^s) = \mathbb{E}_Y(Y \mid A_i^s = a^s, L_i^s = l^s) \quad (\text{Conditional Mean})$$

$$r(a^s, a^{s \circ d^{-1}}, l^s) = \frac{p(a^{s \circ d^{-1}} \mid l^s)}{p(a^s \mid l^s)} \quad (\text{Density Ratio})$$

$$w(\mathbf{a}, \mathbf{l}, i) = \sqrt{\frac{\det J_{\mathbf{a}}(s_{F_i} \circ d^{-1})(\mathbf{a}, \mathbf{l}; \delta) J_{\mathbf{a}}(s_{F_i} \circ d^{-1})(\mathbf{a}, \mathbf{l}; \delta)^\top}{\det J_{\mathbf{a}} s_{F_i}(\mathbf{a}, \mathbf{l}) J_{\mathbf{a}} s_{F_i}(\mathbf{a}, \mathbf{l})^\top}} \quad (\text{Induced MTP Weights})$$

See Supplementary Material S2 for a proof. While m and r are nuisance parameters that must be estimated from the data, w is a deterministic function of the data and the choices of s and d made by the investigator. Since m and r only depend on the summaries of \mathbf{A} and \mathbf{L} , this identification result effectively factorizes the estimand: *all estimation can proceed using exposure and confounder summaries* instead of their individual-level values. Furthermore, while the form of w may appear complex, if s and d are linear, w often simplifies considerably. For example, if $d(a, l; \delta) = \delta \cdot a$ and $s_{F_i}(\mathbf{a}, \mathbf{l}) = \sum_{j \in F_i} \omega_j a_j$ (a weighted sum), then $w(\mathbf{a}, \mathbf{l}, i) = 1/\delta$. Unlike for the estimand of Ogburn et al. (2022), no Monte Carlo procedures are necessary to estimate these nuisance quantities.

3.3 Asymptotically Efficient Estimation

It is well-established that standard plug-in and re-weighting estimators cannot leverage flexible machine learning or non-parametric regression strategies for estimation of nuisance parameters without incurring possibly severe asymptotic bias (Koshevnik & Levit, 1977; Pfanzagl & Wefelmeyer, 1985; Bickel et al., 1993). Constructing a consistent estimator that achieves the semi-parametric efficiency bound—the lowest possible variance among regular asymptotically linear estimators—in the non-parametric model \mathcal{M} requires alternative strategies, for which the efficient influence function is a common ingredient. Such strategies include one-step bias-corrected estimation (Pfanzagl &

Wefelmeyer, 1985; Bickel et al., 1993), unbiased estimating equations (van der Laan & Robins, 2003), targeted maximum likelihood (or minimum loss) estimation (van der Laan & Rubin, 2006; van der Laan & Rose, 2011), and, most recently, double machine learning (Chernozhukov et al., 2018). In many instances, these distinct frameworks yield doubly robust estimators.

We use *doubly robust* to mean that, for nuisances m and r , consistent estimation occurs if the nuisance error product $\|\hat{m} - m\|_2 \|\hat{r} - r\|_2$ is asymptotically negligible. Many common non-parametric regression algorithms can be shown to converge at $n^{1/4}$ rates under certain assumptions (see, e.g., Section 4.3 of Kennedy (2024) or Section 4.1 of Díaz et al. (2021) and references therein). Consequently, when such flexible algorithms are used for nuisance estimation, the product of their convergence rates will be at least $n^{1/2}$ (or faster), making a key second-order remainder term in the von Mises expansion of the estimator and target parameter negligible; moreover, this allows for a doubly robust estimator to achieve consistency under misspecification of either of two nuisance estimators. For a doubly robust estimator to achieve the semi-parametric efficiency bound, both nuisance estimators must be correctly specified (see, e.g., van der Laan & Rose, 2011; Kennedy, 2024).

To construct semi-parametric efficient estimators of ψ_n , we build upon theoretical developments for estimating the causal effect of a stochastic intervention under interference. Assuming the SCM (4), Sofrygin & van der Laan (2017) showed that such a causal effect may be identified as

$$\psi_n^* = \frac{1}{n} \sum_{i=1}^n \int_{\mathcal{L}^s} \int_{\mathcal{A}^s} m(a_i^s, l_i^s) \bar{p}^*(a_i^s | l_i^s) p(l_i^s) \partial \mu(a_i^s, l_i^s), \quad (9)$$

where \bar{p}^* is the mixture of neighbors' conditional exposure distributions that results from replacing each A_i with a random draw A_i^* from some user-specified distribution. As noted by other authors (Young et al., 2014; Díaz & van der Laan, 2018), an MTP may be expressed as a variant of a stochastic intervention whose replacement density depends on A^s and satisfies piecewise smooth invertibility. Consequently, an induced MTP is a stochastic intervention where

$$\bar{p}^*(a_i^s | l_i^s) = p_{A^s}(a_i^{s \circ d^{-1}} | l_i^s) \sqrt{J_{\mathbf{a}}(s_{F_i} \circ d^{-1})(\mathbf{a}, \mathbf{l}; \delta) J_{\mathbf{a}}(s_{F_i} \circ d^{-1})(\mathbf{a}, \mathbf{l}; \delta)^{\top}}, \quad (10)$$

which follows from the change-of-variables formula for functions whose Jacobians $J_{\mathbf{a}}$ are not square. We show this equivalence in Lemma S1 and Section S3 of the Supplementary Material.

The efficient influence function (EIF) for regular asymptotically linear estimators of the statistical functional that identifies the causal effect of a stochastic intervention under interference was first derived by van der Laan (2014). Treating the EIF as an estimating equation is a standard strategy for the construction of semi-parametric efficient estimators (Pfanzagl & Wefelmeyer, 1985; Bickel et al., 1993; van der Laan & Rose, 2011). Applying the representation in Equation (10), we prove in Section S3 of the Supplementary Material that the EIF for the causal effect of an induced MTP is

$$\bar{\phi}_{\mathbf{P}} = \frac{1}{n} \sum_{i=1}^n r(A_i^s, A_i^{s \circ d^{-1}}, L_i^s) w(\mathbf{A}, \mathbf{L}, i) (Y_i - m(A_i^s, L_i^s)) + \mathbb{E}_{\mathbf{P}}[m(A_i^{s \circ d}, L_i^s) | \mathbf{L} = \mathbf{l}] - \psi_n. \quad (11)$$

The EIF $\bar{\phi}_{\mathbf{P}}$ is expressed as an empirical mean because it represents the influence of all n units within the *single draw* of the interference network that is observed. Despite only observing a single realization of the network, it is clear that this EIF is composed of individual i -specific components, with the corresponding EIF estimating equation admitting the expression:

$$\bar{\phi}_{\mathbf{P}} = \frac{1}{n} \sum_{i=1}^n \phi_{\mathbf{P}}(O_i) - \psi_n = 0, \quad (12)$$

where $\phi_{\mathbf{P}}(O_i) = r(A_i^s, A_i^{s \circ d^{-1}}, L_i^s) w(\mathbf{A}, \mathbf{L}, i) (Y_i - m(A_i^s, L_i^s)) + \mathbb{E}_{\mathbf{P}}[m(A_i^{s \circ d}, L_i^s) | \mathbf{L} = \mathbf{l}]$. Ogburn et al. (2022) exploit this structure to prove the following theorem, reproduced for convenience:

Theorem 1 (Central Limit Theorem of Ogburn et al. (2022)). *Suppose an estimator $\hat{\psi}_n$ is a solution to the EIF estimating equation of Equation (12) and that $K_{\max}^2/n \rightarrow 0$ as $n \rightarrow \infty$, where K_{\max} denotes the maximum node degree in the network. Under the SCM (4) and mild regularity conditions, including that the estimating function is bounded,*

$$\sqrt{C_n}(\hat{\psi}_n - \psi_n^*) \xrightarrow{d} N(0, \sigma^2), \quad (13)$$

for some finite σ^2 and some constant C_n such that $n/K_{\max}^2 \leq C_n \leq n$.

This theorem states that if K_{\max} grows asymptotically no faster than $n^{1/2}$, then an estimator $\hat{\psi}_n$ of ψ_n^* attains a normal limiting distribution centered about ψ_n^* . In addition, these authors argue, based on earlier results of van der Laan (2014), that such an estimator of ψ_n^* will exhibit double robustness with respect to the nuisance estimators \hat{m} and \hat{r} , with a second-order remainder term of the form $\|\hat{m} - m\|_2 \|\hat{r} - r\|_2 = o_P(\sqrt{C_n})$, where the estimator $\hat{\psi}_n$ of ψ_n^* remains consistent as long as the rate-product of the differences of the nuisance estimators $\{\hat{m}, \hat{r}\}$ from their respective targets $\{m, r\}$ converges at the specified rate. Since our target estimand ψ_n is equivalent to ψ_n^* under an MTP and appropriate identification conditions, using Theorem 1 and the EIF in Equation (11), we can construct semi-parametric efficient estimators of ψ_n in at least two ways, which we outline next.

One-Step Estimation. A one-step bias-corrected estimator (Pfanzagl & Wefelmeyer, 1985; Bickel et al., 1993) uses Equation (12) to de-bias an initial plug-in estimator by adding to it an estimated $\phi_{\hat{P}_n}(O_i)$, constructed based on nuisance estimators. While we use P_n to denote the empirical distribution, we use \hat{P}_n to denote the empirical distribution augmented by relevant nuisance estimators. The outer expectation in the term $\mathbb{E}_P[\hat{m}(A_i^{sod}, L_i^s) | \mathbf{L} = \mathbf{l}]$ in the EIF can be dropped because the sample means of $\hat{m}(A_i^{sod}, L_i^s)$ and $\mathbb{E}_P[\hat{m}(A_i^{sod}, L_i^s) | \mathbf{L} = \mathbf{l}]$ both converge to the same value (see Section S4 of the Supplementary Material for a proof). Then, the one-step (OS) estimator is

$$\hat{\psi}_n^{\text{OS}} = \frac{1}{n} \sum_{i=1}^n \phi_{\hat{P}_n}(O_i), \quad (14)$$

where $\phi_{\hat{P}_n}(O_i) = \hat{r}(A_i^s, A_i^{sod-1}, L_i^s) w(\mathbf{A}, \mathbf{L}, i) (Y_i - \hat{m}(A_i^s, L_i^s)) + \hat{m}(A_i^{sod}, L_i^s)$. Since the estimating functions are no longer centered, variance estimates must be adjusted (as described in Section 3.5).

Targeted Maximum Likelihood Estimation (TMLE). Although the one-step estimator is semi-parametric efficient, it is not a substitution estimator: it may yield estimates outside the bounds of the parameter space. TMLE—a general template for the construction of substitution estimators that appropriately solve the EIF estimating equation (van der Laan & Rubin, 2006; van der Laan & Rose, 2011)—resolves this shortcoming. Estimation under an induced MTP proceeds as follows:

1. Estimate nuisances functions to obtain $\hat{r}(A_i^s, L_i^s)$, $\hat{r}(A_i^{sod}, L_i^s)$, $\hat{m}(A_i^s, L_i^s)$, and $\hat{m}(A_i^{sod}, L_i^s)$, and compute weights $w(\mathbf{A}, \mathbf{L}, i)$ and $w(\mathbf{A}^d, \mathbf{L}, i)$ from the data based on the chosen s and d .
2. Fit a one-dimensional parametric fluctuation model regressing $\hat{r}(A_i^s, L_i^s) w(\mathbf{A}, \mathbf{L}, i)$ on Y_i with offset $\hat{m}(A_i^s, L_i^s)$; a common choice for this is logistic regression $\text{logit}(Y_i) = \text{logit}(\hat{m}(A_i^s, L_i^s)) + \varepsilon \hat{r}(A_i^s, L_i^s) w(\mathbf{A}, \mathbf{L}, i)$, where the Y_i are rescaled to ensure each lies in the open unit interval $(0, 1)$.
3. Compute $\hat{m}^*(A_i^{sod}, L_i^s) = \text{expit}(\text{logit}(\hat{m}(A_i^{sod}, L_i^s)) + \hat{\varepsilon} \hat{r}(A_i^{sod}, L_i^s) w(\mathbf{A}^d, \mathbf{L}, i))$ if using the logistic fluctuation model, or more broadly, compute the corresponding parametric fluctuation model predictions under the MTP intervention, based on the MLE $\hat{\varepsilon}$ of ε .
4. Compute the TML estimate as $\hat{\psi}_n^{\text{TMLE}} = \frac{1}{n} \sum_{i=1}^n \hat{m}^*(A_i^{sod}, L_i^s)$.

In Step 2, the corresponding estimate $\hat{\varepsilon}$ is used to fluctuate the initial estimator $\hat{m}(A_i^s, L_i^s)$, using the summary-weighted density ratio $\hat{r}(A_i^s, L_i^s) w(\mathbf{A}, \mathbf{L}, i)$, to an updated version $\hat{m}^*(A_i^s, L_i^s)$ in such a way that the EIF estimating equation is solved. Logistic regression is commonly employed to guarantee each prediction \hat{m}^* falls in the bounds of the parameter space, thus respecting global constraints (Gruber & van der Laan, 2010). One can also fit an intercept-only model with $\hat{r}(A_i^s, L_i^s) w(\mathbf{A}, \mathbf{L}, i)$ as weights themselves, which may improve stability. In what follows, we refer to this estimator as “network-TMLE,” following nomenclature introduced by Zivich et al. (2022), who discuss its use in practical settings and examine its properties in simulation experiments.

3.4 Nuisance Parameter Estimation

The underlying form of nuisance parameters m and r is usually recognized as being unknown and may involve, for example, complex nonlinear interactions between covariates. Therefore, it is desirable to estimate such quantities using flexible regression or machine learning approaches. This process often employs K -fold cross-fitting (Zheng & van der Laan, 2010; Chernozhukov et al., 2018) to eliminate asymptotic bias arising from empirical process terms (Pfanzagl & Wefelmeyer, 1985; Klaassen, 1987).

Perhaps surprisingly, the form of cross-fitting used for independent units still accomplishes the same goals even in our network setting. That is, splitting the data into K folds, fitting nuisance functions on each combination of $K - 1$ folds, and obtaining out-of-sample predictions for each held-out fold is sufficient to render any empirical process bias asymptotically negligible, even when units may be correlated according to Equation 4. A formal proof can be found

in Section S6 of the Supplementary Material. At a high level, it follows similarly to an m -dependence argument: a sample mean is unbiased even under dependence, and its variance will shrink at a rate dependent on the maximum degree of the network, which in our setting is limited by assumption. The result mirrors similar numerical findings in the longitudinal data setting (e.g., Fuhr & Papies, 2024). Consequently, cross-fitting can be performed identically whether units may be independent or correlated according to a network whose maximum degree grows according to Theorem 1.

Since the outcome regression m is a conditional expectation function, it can be estimated using any supervised learning algorithm. We recommend super learning (van der Laan et al., 2007), that is, fitting an ensemble of candidate regression algorithms in a cross-validated manner and selecting the candidate yielding the lowest cross-validated risk (for continuous outcomes, we use mean-squared error). This guarantees that the selected algorithm performs asymptotically as well as the best candidate algorithm in the library used to construct the ensemble (van der Laan et al., 2004; van der Vaart et al., 2006), even in the fixed regression design setting presently considered (Davies & van der Laan, 2016). Phillips et al. (2023) proposed guidance and heuristics to aid in overcoming the considerable challenge of assembling a candidate library from the diversity of learning algorithms available.

An advantage of the MTP framework is that the implied form of the intervention, unlike general stochastic interventions (Díaz & van der Laan, 2012; Sofrygin & van der Laan, 2017; Ogburn et al., 2022), facilitates direct estimation of the density ratio r , circumventing the need to learn a conditional density function. A common density ratio estimator is based on probabilistic classification (Qin, 1998; Cheng & Chu, 2004), in which a classifier is trained to distinguish between natural and intervened samples, and its output is transformed into a density ratio using Bayes' rule. The use of this method with an MTP is described in detail by Díaz et al. (2023, see Section 5.4). We recommend super learning with binary log loss to select the optimal classifier. One can also employ kernel-based methods, including kernel mean matching, Kullback-Leibler importance estimation, and least-squares importance fitting, as outlined in detail by Sugiyama et al. (2012).

3.5 Variance Estimation

Summary measures are correlated if they aggregate the same neighboring units. As a result, the as-iid sample variance of the estimated EIF will be conservative, especially if the network degree distribution is highly skewed (Sofrygin & van der Laan, 2017). A consistent variance estimator for the solution to an arbitrary estimating equation $\frac{1}{n} \sum_{i=1}^n \varphi_i = 0$ with a centered estimating function φ_i satisfying $\mathbb{E}[\varphi_i] = 0$ is given by

$$\hat{\sigma}^2 = \frac{1}{n^2} \sum_{i,j} G(i,j) \varphi_i \varphi_j, \quad (15)$$

where $G(i,j) = 1$ if $i = j$, i and j are in each others' dependency neighborhoods, or i and j share a friend k , and $G(i,j) = 0$ otherwise. A useful feature of $\hat{\sigma}^2$ is that it automatically incorporates the scaling factor C_n based on the CLT of Ogburn et al. (2022). Intuitively, this is because $\hat{\sigma}^2$ includes n "variance" terms φ_i^2 , as well as a certain number of "covariance" terms $\varphi_i \varphi_j$ (for $i \neq j$), the number of which scales with $n/K_{\max}^2 \leq C_n \leq n$, representing the rate of connectivity in the network. Consequently, $(1 - \alpha)\%$ Wald-style confidence intervals can be constructed via the standard approach: $\hat{\psi}_n \pm \Phi^{-1}(\alpha/2) \sqrt{\hat{\sigma}^2/n}$, where Φ is the CDF of the standard normal distribution.

As the estimators from Section 3.3 are constructed based on the *uncentered* estimating function $\phi_{\mathbb{P}}(O_i)$, this result does not transport directly to our setting. However, examining the SCM (4) reveals that O_i and O_j will be identically distributed and therefore have the same mean provided that they have the same number of neighbors, that is, $|F_i| = |F_j|$. Following a similar strategy as Emmenegger et al. (2025), a centered estimating function is $\phi_{\mathbb{P}}(O_i) - \hat{\psi}_n(|F(O_i)|)$, where $\hat{\psi}_n(|F(O_i)|)$ denotes the mean of $\phi_{\mathbb{P}}(O_j)$ over all units in $j \in 1, \dots, n$, satisfying the equality $|F_j| = |F_i|$. This centering term can be estimated by computing $\hat{\psi}_n^{\text{OS}}$ within each subgroup of possible $|F_i|$. Formally, this is

$$\hat{\psi}_n(|F_i|) = \frac{1}{|\mathcal{N}(|F_i|)|} \sum_{j \in \mathcal{N}(|F_i|)} \phi_{\mathbb{P}_n}(O_j), \quad (16)$$

where $\mathcal{N}(m) = \{k : k \in 1, \dots, n, |F_k| = m\}$. Then, letting $\varphi_i = \phi_{\mathbb{P}_n}(O_i) - \hat{\psi}_n(|F_i|)$, the estimator $\hat{\sigma}^2$ in Equation (15) consistently estimates the variances of $\hat{\sigma}_n^{\text{OS}}$ and $\hat{\sigma}_n^{\text{TMLE}}$, provided both nuisance estimators are consistent for their targets (see Supplementary Material, Section S5, for a proof).

4 Results: Numerical Experiments

We now empirically evaluate the estimators described in Section 3. All data in this section are simulated in the numerical computing language `Julia` (Bezanson et al., 2017), using the package `CausalTables.jl` (Balkus &

Hejazi, 2025). MTP estimates are computed using `ModifiedTreatment.jl` (Balkus & Hejazi, 2024), a Julia package implementing the estimators described in this work. Unless otherwise specified, conditional means and density ratios are estimated using super learning—from an ensemble consisting of a GLM, random forest, and multiple gradient boosted tree models with various sets of hyperparameters—to select the algorithm minimizing the cross-validated empirical risk with respect to an appropriate loss (MSE for the conditional mean, binary log-loss for the density ratio). Code for these experiments and the data analysis is available on GitHub at <https://github.com/salbalkus/pub-code-mtp-interfere>.

4.1 Results of Experiments with Synthetic Data

First, we evaluate estimators on simulated data with both network interference and nonlinear relationships between confounders, exposure, and outcome. We simulate this data using three common network structures: Erdős-Rényi (with $p = 3/n$), static scale-free (with $\lambda = 3.5$), and Watts-Strogatz (with $K = 6$ and $\beta = 0.5$). Data are generated according to the following set of structural equations:

$$\begin{aligned} \mathbf{L}_1 &\sim \text{Beta}(3, 2); \mathbf{L}_2 \sim \text{Poisson}(100); \mathbf{L}_3 \sim \text{Gamma}(2, 4); \mathbf{L}_4 \sim \text{Bernoulli}(0.6) \\ m_L &= \left(1 + L_4\right) \cdot \left(-2(\mathbb{I}(L_1 > 0.3) + \mathbb{I}(L_2 > 90) + \mathbb{I}(L_3 > 5)) - (\mathbb{I}(L_1 > 0.5) + \mathbb{I}(L_2 > 100) + \mathbb{I}(L_3 > 10)) + 2(\mathbb{I}(L_1 > 0.7) + \mathbb{I}(L_2 > 110) + \mathbb{I}(L_3 > 15))\right) \\ \mathbf{A} &\sim \text{Normal}(m_L - 5, 1.0) \text{ and } \mathbf{A}^s = \left[\sum_{j \in F_i} A_i\right]_{i=1}^n \\ m_A &= -2\mathbb{I}(A > -2) - \mathbb{I}(A > 1) + 3\mathbb{I}(A > 3); m_{A_s} = 3\mathbb{I}(A_s > 0) + \mathbb{I}(A_s > 6) + \mathbb{I}(A_s > 12) \\ \mathbf{Y} &\sim \text{TruncNormal}(m_L \cdot (1 + 0.2m_A + m_{A_s}) + 5, 2.0), \end{aligned}$$

where `TruncNormal` denotes a normal distribution truncated at six standard deviations. We estimate the counterfactual mean under the MTP $d(a, l) = a + 0.25$ using network-TMLE. Being very similar, one-step estimator results are omitted for brevity.

Figure 2 demonstrates how the empirical performance of our estimator using network-TMLE aligns with theoretical results outlined in Section 3. Bias reliably converges towards zero with increasing sample size across all three network structures, and is highest for scale-free, the network with the most skewed distribution of node degree. Since K_{\max} in each network grows at roughly $\log(n)$ or slower, we use $\sqrt{C_n} = \sqrt{n}/\log(n)$ as a scaling factor for the scaled bias and MSE; these values still decrease, so we can conclude that the convergence rate of network-TMLE matches the expected rate. MSE converges to the efficiency bound; see Supplementary Material S7.1 for details on this bound. The MSE is highest in the Watts-Strogatz simulation, whose network has the highest average node degree (and thus the greatest correlation between units)—hence, a denser network increases variance. Furthermore, the coverage rate of the 95% confidence interval approaches the nominal level for all three graphs. Based on these observations, we conclude that the network-TMLE estimator performs as expected (see Supplementary Material S7.2 for a comparison to classical methods).

4.2 Results of Experiments with Semi-Synthetic Data

In a second simulation experiment, we generate semi-synthetic data based on the real-world dataset that inspired this work and that is analyzed in Section 5. Sixteen normalized confounding variables are taken as fixed covariates, with the 2013 and 2019 LODES commuting pattern data (U.S. Census Bureau, 2024) for California as the network profile \mathbf{F} . From these, we draw exposure and outcome from normal distributions with means following a linear function of the confounders and A^s , a trimmed sum of neighbors' values of A over neighbors that contributed at least 2.5% of commuters into the given unit. These are represented by structural equations, conditional on \mathbf{L} and \mathbf{F} , expressed as

$$\begin{aligned} \mathbf{L}_k^s &= \left[\sum_{j \in F_i} L_{k,i}\right]_{i=1}^n \quad \mathbf{A} \sim \text{Normal}\left(\sum_{k=1}^{16} \mathbf{L}_k - 50, 1.0\right) \text{ and } \mathbf{A}^s = \left[\sum_{j \in F_i} A_i\right]_{i=1}^n \\ \mathbf{Y} &\sim \text{TruncNormal}\left(\mathbf{A} + \mathbf{A}^s + \sum_{k=1}^{16} \mathbf{L}_k + \sum_{k=1}^{16} \mathbf{L}_k^s - 50, 1.0\right), \end{aligned} \tag{17}$$

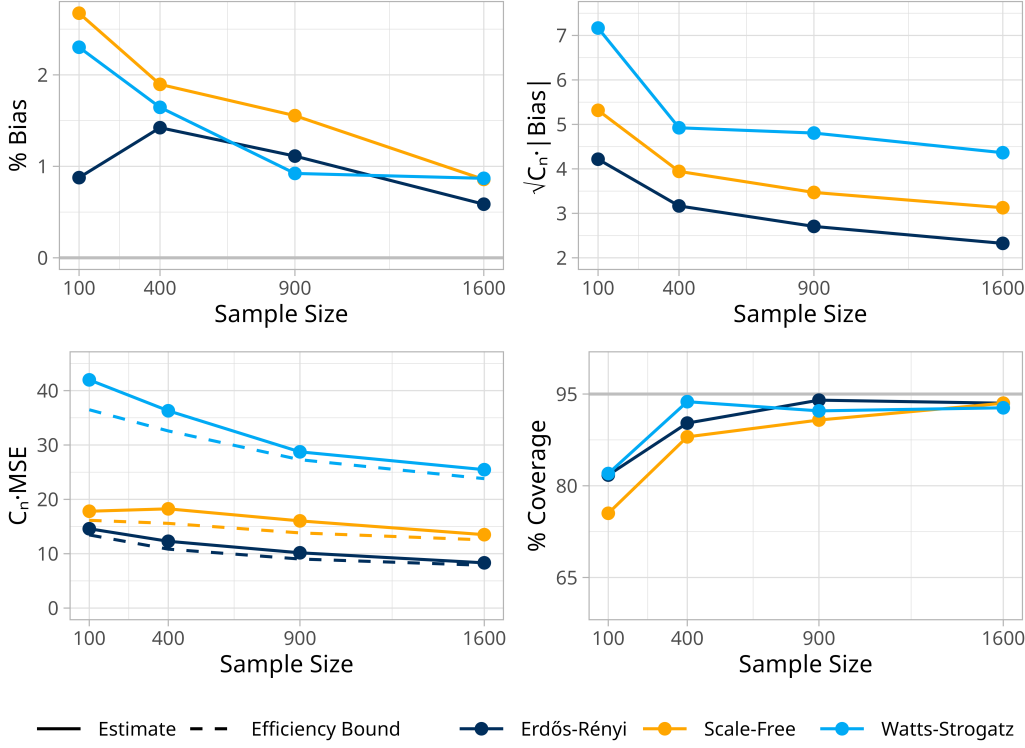


Figure 2: Asymptotic performance of network-TMLE in simulation on multiple network structures.

We estimate the population causal effect of an MTP in 400 simulations using four different estimators: network-TMLE with correctly-specified GLMs (linear regression for the outcome regression and logistic regression for the density ratio probabilistic classifier), network-TMLE with super learning for both nuisance estimators, IID-TMLE with correctly-specified GLMs, and main-terms linear regression. In this simulation, $n = 1652$, the same as in the dataset considered in Section 5.

Table 1 depicts the operating characteristics of the estimators. It is clear from inspection that accounting for network interference can yield dramatically lower bias, even when the outcome regression is otherwise correctly specified. In this case, using network-TMLE with a correctly specified GLM decreased the mean percent bias from over 20% to about 0.1%, and cut variance by about 25%. Even if super learning is used, the mean percent bias of the network-TMLE remains relatively low, at around 1%, and the variance is approximately identical. Furthermore, confidence interval coverage for the network-TMLE is close to nominal under both configurations of nuisance estimators. Alternative methods suffer greatly reduced coverage due to their severe bias.

Table 1: Network-TMLE performance on semi-synthetic data versus competing estimators

Method	Learner	Bias (%)	Variance	Coverage (%)	CI Width
Network TMLE	Correct GLM	0.11	1.56	96.2	4.88
	Super Learner	1.03	1.56	94.0	4.88
Classical TMLE	Correct GLM	20.43	2.11	54.8	5.70
Linear Regression	Correct GLM	20.62	2.12	55.0	5.71

5 Illustrative Data Analysis: Mobile Source Air Pollution

In this section, we use induced MTPs to analyze the causal effect of “zero-emissions” vehicle (ZEV) uptake in California on NO_2 air pollution using observational data. NO_2 is a byproduct of gasoline-powered vehicles shown to be

associated with adverse health outcomes, including respiratory issues and mortality (Hesterberg et al., 2009; Gillespie-Bennett et al., 2010; Faustini et al., 2014). In the U.S., national ambient air quality standards (NAAQs) are set by the Environmental Protection Agency (EPA) to limit the amount of allowable NO_2 in the air (U.S. Environmental Protection Agency, 2018).

5.1 Applied Science Background and Motivations

As ZEVs do not produce tailpipe emissions, governments have heavily promoted their adoption to limit air pollution. State governments must ascertain whether these policies work as intended; hence, understanding how much localized air pollution has decreased as a result of increased ZEV adoption is of both scientific and policy interest. Garcia et al. (2023) analyzed whether ZEV uptake was associated with NO_2 air pollution across ZIP code tabulation areas (ZCTA) in California from 2013 to 2019. They found that an increase of 20 ZEVs per 1000 population units was associated with a reduction of 0.41 parts per billion in NO_2 within a given ZCTA on average; however, with a p -value of 0.252 and confidence interval of $(-1.12, 0.29)$, this finding was far from statistically significant.

This is a problem in which network interference arises as a result of people driving outside the ZCTA in which they reside; that is, individuals commute in their vehicles to other ZCTAs, emitting pollution there as well. Garcia et al. (2023) controlled for confounding using linear regression, without accounting for interference due to individuals commuting in vehicles from one ZCTA unit to another. As evidenced by our simulation experiments in Section 4, neglecting interference can induce bias and yield misleading confidence intervals. In addition, overreliance on restrictive parametric modeling may be cause for concern, as linearity imposes a strict functional form which may not adequately capture the underlying complexity, resulting in model misspecification bias. The goal of our data analysis is to study the same research question as Garcia et al. (2023) and compare how flexibly evaluating the causal effect of an induced MTP can improve inference in this setting.

5.2 Estimation Strategy

Following Garcia et al. (2023), we compute the exposure, the percentage of light-duty vehicles in California actively registered as ZEVs by April 2019, for each ZCTA from the California Energy Commission (2024). The outcome, change in NO_2 from 2013 to 2019 in parts per billion (ppb), is spatially aggregated from a 1 km grid of estimated pollution levels (Cooper, 2022a,b); this provides finer-grain ZCTA-level estimates than the raw sensor data used by Garcia et al. (2023). Socioeconomic confounders are accessed from the U.S. Census via Walker & Herman (2024), while land-use confounders are obtained from the U.S. Environmental Protection Agency (2024); see Section S7 of the Supplementary Material for summary statistics. We performed spatial alignment and areal weighted interpolation of missing values using the `sf` (Pebesma, 2018) and `areal` (Prener et al., 2019) packages in the `R` language for statistical computing and graphics (R Core Team, 2025).

Finally, to account for interference, we rely on commuting networks describing the number of people traveling between home and work ZCTAs (de Souza et al., 2023; U.S. Census Bureau, 2024). The induced MTP summary estimates the percentage of incoming work commuters driving ZEVs during the 2013–2019 time period, as used for the outcome. This was computed by summing the percentage of ZEVs in each neighboring ZCTA in each year’s network, with each unit’s summand weighted by the percentage of its neighbor’s population who drive to work and normalized. Sums of neighboring covariates are also included as potential confounders for the induced MTP.

We compared the following data-analytic strategies: (1) estimating an induced MTP using network-TMLE, (2) estimating a classical MTP using IID-TMLE, and (3) estimating a main-terms GLM regression coefficient. Each seeks to answer the same question: “how much *more* would average NO_2 have decreased from 2013 to 2019 had each ZCTA experienced an increase in the percentage of vehicles registered as ZEV by 2019?” Strategy (1) accounts for interference and estimates nuisances using flexible super learning. Strategy (2) uses super learning but ignores interference. Strategy (3) imposes a strict linearity assumption and ignores interference. Both super learning procedures selected random forest for the outcome regression and density ratio probabilistic classifier.

5.3 Analytic Results

Figure 3 displays the three estimates of additive and multiplicative effects of an MTP increasing the proportion of ZEVs. According to the induced MTP effect estimate, adding 1% to the proportion of ZEVs across ZCTAs would be expected to yield a 0.044 ppb decrease in NO_2 on average. This estimate is over 1.3 times larger than the MTP effect estimate arrived at when not accounting for interference (0.032 ppb), and about 2.8 times larger than the GLM-based estimate (0.015 ppb). Similarly, the induced MTP effect estimate indicated that scaling the proportion of ZEVs by 20% across ZCTAs would be expected to yield a 0.048 ppb decrease in NO_2 on average—over 1.4 times larger

than the naive MTP effect estimate (0.033 ppb) and the GLM-based estimate (0.027 ppb). Interpreted in a scientific context, for the additive shift, the estimated effect based on the induced MTP indicates that ZEV uptake would have accounted for about 7% of the overall mean decrease in NO_2 from 2013-2019, whereas a GLM-based estimate would have accounted for only 2.5%.

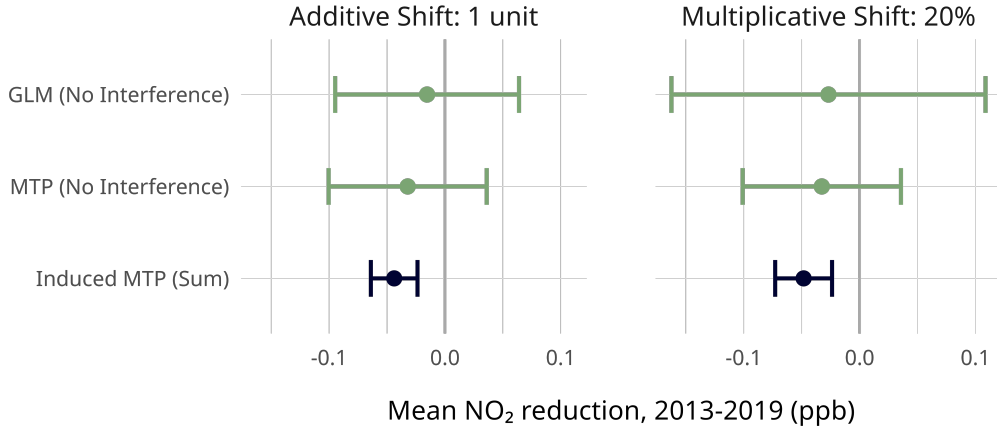


Figure 3: Estimated effect sizes measuring the expected difference in NO_2 across California ZCTAs caused by two different increases in the proportion of ZEVs in 2019.

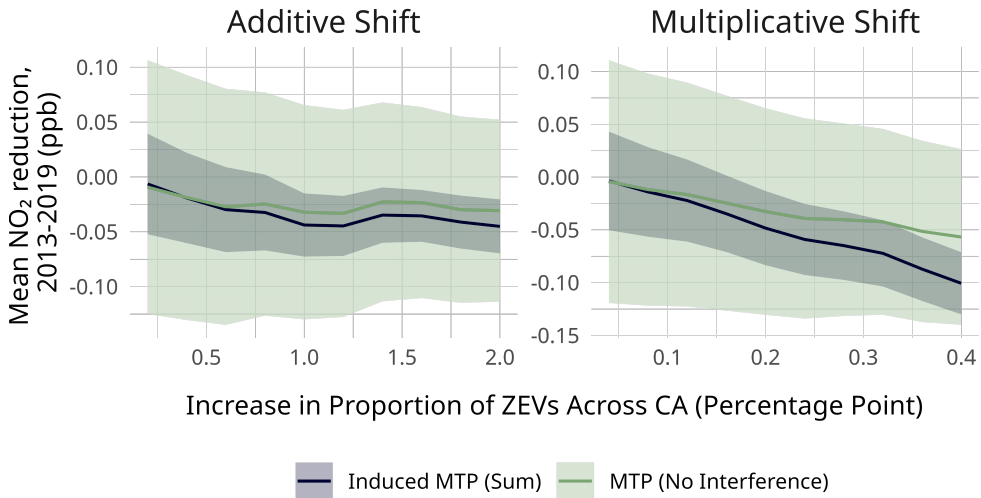


Figure 4: Estimated effect sizes measuring the expected difference in NO_2 across California ZCTAs caused by various additive or multiplicative shifts in the percentage of ZEVs in 2019. Confidence bands use a conservative Bonferroni multiplicity correction.

Accounting for interference and using flexible regression yielded larger effect estimates than those recovered by classical analyses, suggesting commuting contributes significantly to vehicular NO_2 pollution. This was especially pronounced for the multiplicative shift, indicating that ZCTAs with many out-commuters exacerbate NO_2 . Furthermore, while one might expect that accounting for interference would yield wider confidence intervals due to correlation between units, we observe the opposite—drastically lower variance. We conjecture that improvements in estimation of the outcome regression drive this result, as including exposure summaries as covariates reduces model misspecification, allowing the model to explain a larger proportion of the outcome variance.

Figure 4 displays effect estimates over a grid of possible additive and multiplicative shifts. At low-magnitude shifts, the estimates were roughly the same. However, at larger shifts—about 0.75% on the additive scale and 10% on the multiplicative scale—the estimated effects diverged, with those accounting for interference becoming more pronounced. The trend was also less erratic under the multiplicative shift, possibly because it only produces a large shift

among ZCTAs with a large proportion of ZEVs, thereby avoiding destabilizing empirical positivity issues. Such a result highlights the importance of considering MTPs that can be easily estimated from the data available.

Our analysis focused on NO_2 since it is a well-understood pollutant. That said, from 2013–2019, average NO_2 levels changed little across ZCTAs, as all ZCTAs within California have remained well within limits regarded as safe based on EPA guidance (U.S. Environmental Protection Agency, 2018), so the effects are inherently small. However, suppose policymakers sought further reductions and would impose a ZEV-promoting policy given statistically significant evidence. Then, according to Figures 3 and 4, evidence from an induced MTP would have resulted in imposing a ZEV-promoting policy ($p < 0.05$) versus not imposing such a policy ($p > 0.05$) if interference was ignored. Hence, our method provides much stronger and more conclusive evidence regarding even the small effect sizes in this setting.

6 Discussion

In this work, we introduced the induced modified treatment policy, a new class of MTP that accounts for known network interference. This intervention is useful for causal inference in observational data settings that feature continuous exposures and network interference. We established identification of the causal effect of an induced MTP using a novel application of the coarea formula and outlined procedures for constructing semi-parametric-efficient estimators capable of incorporating flexible nuisance estimation strategies via, for example, machine learning or non-parametric regression.

Using simulation experiments, we showed that interference can result in significant bias when it is not corrected using an induced MTP. Our illustrative data analysis demonstrates the perils of ignoring interference and applying restrictive parametric modeling strategies with observational spatial data, as is often done in environmental epidemiology and related fields. Such oversimplifications can suggest starkly different scientific conclusions than those provided by our proposed strategy.

In practice, several challenges remain. One limitation is that ratios of conditional densities are still more difficult to estimate than conditional expectation functions, especially in high-dimensional settings (Sugiyama et al., 2012). This problem is exacerbated under interference: for units with an excessively large number of neighbors, the density ratio between the natural and post-intervention exposure could grow extremely large, destabilizing downstream estimates. More modern “balancing” tools, such as Riesz regression (Chernozhukov et al., 2021), may help overcome this issue.

In addition, practitioners must know how the interference arises. This does often occur: in our data analysis, the form of interference arose naturally as a part of the scientific question that considered an intervention on *all* vehicles entering a given ZCTA, not just those registered there. If an investigator has reason to suspect interference, they may also suspect the underlying process by which it occurs. However, there are cases where an investigator may not know the form. Although discussed in recent work (Hoshino & Yanagi, 2023; Ohnishi et al., 2022), this remains an avenue for future research.

Other potential areas of future research involve extending the induced MTP to more complex settings. In time-varying data, for example, one might consider using an *induced longitudinal* MTP (Díaz et al., 2023), which would involve sequential regression-based algorithms to account for summary measures of exposures subject to time-varying confounding in a network profile that may itself evolve across time. Further work overcoming the technical limitations of estimating the effects of induced MTPs will be critical to facilitate answering more complex causal inference questions in settings where continuous exposures are measured in datasets exhibiting network interference.

Acknowledgments

SVB was supported in part by grants from the National Institute of Environmental Health Sciences (award no. T32 ES007142) and the National Science Foundation (award no. DGE 2140743). The authors thank Rachel Nethery for her help in initiating the motivating data analysis.

Conflicts of interest: The authors have no conflicts of interest to disclose.

References

ARONOW, P. M. & SAMII, C. (2017). Estimating average causal effects under general interference, with application to a social network experiment. *The Annals of Applied Statistics* **11**, 1912–1947.

ATHEY, S., ECKLES, D. & IMBENS, G. W. (2017). Exact p-values for network interference. *Journal of the American Statistical Association* **113**, 230–240.

BALKUS, S. & HEJAZI, N. (2024). ModifiedTreatment.jl. <https://github.com/salbalkus/ModifiedTreatment.jl>.

BALKUS, S. V. & HEJAZI, N. S. (2025). Causaltables.jl: Simulating and storing data for statistical causal inference in Julia. *Journal of Open Source Software* **10**, 7580.

BEZANSON, J., EDELMAN, A., KARPINSKI, S. & SHAH, V. B. (2017). Julia: A fresh approach to numerical computing. *SIAM Review* **59**, 65–98.

BICKEL, P. J., KLAASSEN, C. A., BICKEL, P. J., RITOY, Y., KLAASSEN, J., WELLNER, J. A. & RITOY, Y. (1993). *Efficient and adaptive estimation for semiparametric models*, vol. 4. Springer.

CALIFORNIA ENERGY COMMISSION (2024). Light-duty vehicle population in California .

CHENG, K. & CHU, C. (2004). Semiparametric density estimation under a two-sample density ratio model. *Bernoulli* **10**.

CHERNOZHUKOV, V., CHETVERIKOV, D., DEMIRER, M., DUFLO, E., HANSEN, C., NEWHEY, W. & ROBINS, J. (2018). Double/debiased machine learning for treatment and structural parameters. *The Econometrics Journal* **21**, C1–C68.

CHERNOZHUKOV, V., NEWHEY, W. K., QUINTAS-MARTINEZ, V. & SYRGKANIS, V. (2021). Automatic debiased machine learning via Riesz regression. *arXiv:2104.14737* .

CLARK, D. A. & HANDCOCK, M. S. (2024). Causal inference over stochastic networks. *Journal of the Royal Statistical Society Series A: Statistics in Society* **187**, 772–795.

COOPER, M. (2022a). Satellite-derived ground level NO₂ concentrations, 2005–2019.

COOPER, M. (2022b). Tropomi-derived ground level NO₂ concentrations (2019 annual mean).

COX, D. R. (1958). Planning of experiments. .

DAVIES, M. M. & VAN DER LAAN, M. J. (2016). Optimal spatial prediction using ensemble machine learning. *The International Journal of Biostatistics* **12**, 179–201.

DE SOUZA, P., ANENBERG, S., MAKAREWICZ, C., SHIRGAOKAR, M., DUARTE, F., RATTI, C., DURANT, J. L., KINNEY, P. L. & NIEMEIER, D. (2023). Quantifying disparities in air pollution exposures across the United States using home and work addresses. *Environmental Science & Technology* **58**, 280–290.

DÍAZ, I. & HEJAZI, N. S. (2020). Causal mediation analysis for stochastic interventions. *Journal of the Royal Statistical Society: Series B (Statistical Methodology)* **82**, 661–683.

DÍAZ, I., HEJAZI, N. S., RUDOLPH, K. E. & VAN DER LAAN, M. J. (2021). Non-parametric efficient causal mediation with intermediate confounders. *Biometrika* **108**, 627–641.

DÍAZ, I., HOFFMAN, K. L. & HEJAZI, N. S. (2024). Causal survival analysis under competing risks using longitudinal modified treatment policies. *Lifetime Data Analysis* **30**, 213–236.

DÍAZ, I. & VAN DER LAAN, M. (2012). Population intervention causal effects based on stochastic interventions. *Biometrics* **68**, 541–549.

DÍAZ, I. & VAN DER LAAN, M. J. (2018). Stochastic treatment regimes. In *Targeted Learning in Data Science: Causal Inference for Complex Longitudinal Studies*. Springer Science & Business Media, pp. 167–180.

DÍAZ, I., WILLIAMS, N., HOFFMAN, K. L. & SCHENCK, E. J. (2023). Nonparametric causal effects based on longitudinal modified treatment policies. *Journal of the American Statistical Association* **118**, 846–857.

ELLIOTT, P. & WARTENBERG, D. (2004). Spatial epidemiology: Current approaches and future challenges. *Environmental Health Perspectives* **112**, 998–1006.

EMMENEGGER, C., SPOHN, M.-L., ELMER, T. & BÜHLMANN, P. (2025). Treatment effect estimation with observational network data using machine learning. *Journal of Causal Inference* **13**.

FAUSTINI, A., RAPP, R. & FORASTIERE, F. (2014). Nitrogen dioxide and mortality: review and meta-analysis of long-term studies. *European Respiratory Journal* **44**, 744–753.

FUHR, J. & PAPIES, D. (2024). Double machine learning meets panel data – promises, pitfalls, and potential solutions. *arXiv:2409.01266* .

GARCIA, E., JOHNSTON, J., MCCONNELL, R., PALINKAS, L. & ECKEL, S. P. (2023). California's early transition to electric vehicles: Observed health and air quality co-benefits. *Science of The Total Environment* , 161761.

GILBERT, B., HOFFMAN, K. L., WILLIAMS, N., RUDOLPH, K. E., SCHENCK, E. J. & DÍAZ, I. (2024). Identification and estimation of mediational effects of longitudinal modified treatment policies. *arXiv:2403.09928*.

GILLESPIE-BENNETT, J., PIERSE, N., WICKENS, K., CRANE, J. & HOWDEN-CHAPMAN, P. (2010). The respiratory health effects of nitrogen dioxide in children with asthma. *European Respiratory Journal* **38**, 303–309.

GRUBER, S. & VAN DER LAAN, M. J. (2010). A targeted maximum likelihood estimator of a causal effect on a bounded continuous outcome. *The International Journal of Biostatistics* **6**.

HALLORAN, M. E. & HUGGENS, M. G. (2016). Dependent happenings: A recent methodological review. *Current Epidemiology Reports* **3**, 297–305.

HANEUSE, S. & ROTNITZKY, A. (2013). Estimation of the effect of interventions that modify the received treatment. *Statistics in Medicine* **32**, 5260–5277.

HEJAZI, N. S., DÍAZ, I. & VAN DER LAAN, M. J. (2022). Efficient estimation of modified treatment policy effects based on the generalized propensity score. *arXiv:2205.05777*.

HEJAZI, N. S., RUDOLPH, K. E., VAN DER LAAN, M. J. & DÍAZ, I. (2023). Nonparametric causal mediation analysis for stochastic interventional (in)direct effects. *Biostatistics* **24**, 686–707.

HESTERBERG, T. W., BUNN, W. B., MCCLELLAN, R. O., HAMADE, A. K., LONG, C. M. & VALBERG, P. A. (2009). Critical review of the human data on short-term nitrogen dioxide (NO₂) exposures: Evidence for NO₂ no-effect levels. *Critical Reviews in Toxicology* **39**, 743–781.

HOFFMAN, K. L., SALAZAR-BARRETO, D., WILLIAMS, N. T., RUDOLPH, K. E. & DÍAZ, I. (2024). Studying continuous, time-varying, and/or complex exposures using longitudinal modified treatment policies. *Epidemiology* **35**, 667–675.

HOSHINO, T. & YANAGI, T. (2023). Causal inference with noncompliance and unknown interference. *Journal of the American Statistical Association* , 1–12.

HUBBARD, A. E., KHERAD-PAJOUH, S. & VAN DER LAAN, M. J. (2016). Statistical inference for data adaptive target parameters. *The International Journal of Biostatistics* **12**, 3–19.

HUGGENS, M. G. & HALLORAN, M. E. (2008). Toward causal inference with interference. *Journal of the American Statistical Association* **103**, 832–842.

KENNEDY, E. H. (2024). Semiparametric doubly robust targeted double machine learning: A review. In *Handbook of Statistical Methods for Precision Medicine*, E. Laber, B. Chakraborty, E. E. M. Moodie, T. Cai & M. J. van der Laan, eds. Chapman and Hall/CRC, pp. 207–236.

KLAASSEN, C. A. J. (1987). Consistent estimation of the influence function of locally asymptotically linear estimators. *The Annals of Statistics* , 1548–1562.

KOSHEVNIK, Y. A. & LEVIT, B. Y. (1977). On a non-parametric analogue of the information matrix. *Theory of Probability & Its Applications* **21**, 738–753.

LIU, J., ZHANG, D. & TCHETGEN TCHETGEN, E. J. (2025). Auto-doubly robust estimation of causal effects on a network. *arXiv:2506.23332*.

MORRISON, C. N., MAIR, C. F., BATES, L., DUNCAN, D. T., BRANAS, C. C., BUSHOVER, B. R., MEHRANBOD, C. A., GOBAUD, A. N., UONG, S., FORREST, S., ROBERTS, L. & RUNDLE, A. G. (2024). Defining spatial epidemiology: A systematic review and re-orientation. *Epidemiology* .

NEGRO, L. (2022). Sample distribution theory using coarea formula. *Communications in Statistics - Theory and Methods* **53**, 1864–1889.

OGBURN, E. L., SOFRYGIN, O., DÍAZ, I. & VAN DER LAAN, M. J. (2022). Causal inference for social network data. *Journal of the American Statistical Association* , 1–15.

OHNISHI, Y., KARMAKAR, B. & SABBAGHI, A. (2022). Degree of interference: A general framework for causal inference under interference. *arXiv:2210.17516* .

PEARL, J. (2000). Causality: Models, reasoning and inference. *Cambridge University Press* **19**, 3.

PEARL, J. (2010). On the consistency rule in causal inference: Axiom, definition, assumption, or theorem? *Epidemiology* **21**, 872–875.

PEBESMA, E. (2018). Simple Features for R: Standardized Support for Spatial Vector Data. *The R Journal* **10**, 439–446.

PFANZAGL, J. & WEFELMEYER, W. (1985). Contributions to a general asymptotic statistical theory. *Statistics & Risk Modeling* **3**, 379–388.

PHILLIPS, R. V., VAN DER LAAN, M. J., LEE, H. & GRUBER, S. (2023). Practical considerations for specifying a super learner. *International Journal of Epidemiology* **52**, 1276–1285.

PRENER, CHRISTOPHER, REVORD & CHARLES (2019). areal: An R package for areal weighted interpolation. *Journal of Open Source Software* **4**.

QIN, J. (1998). Inferences for case-control and semiparametric two-sample density ratio models. *Biometrika* **85**, 619–630.

R CORE TEAM (2025). *R: A Language and Environment for Statistical Computing*. R Foundation for Statistical Computing, Vienna, Austria.

REICH, B. J., YANG, S., GUAN, Y., GIFFIN, A. B., MILLER, M. J. & RAPPOLD, A. (2021). A review of spatial causal inference methods for environmental and epidemiological applications. *International Statistical Review* **89**, 605–634.

ROBINS, J. M., HERNÁN, M. & SIEBERT, U. (2004). Effects of multiple interventions. In *Comparative Quantification of Health Risks: Global and Regional Burden of Disease Attributable to Selected Major Risk Factors*, M. Ezzati, A. D. Lopez, A. Rodgers & M. C. J. L, eds. World Health Organization.

RUBIN, D. B. (1980). Randomization analysis of experimental data: The fisher randomization test comment. *Journal of the American Statistical Association* **75**, 591–593.

SARVET, A. L. & STENSRUD, M. J. (2025). The natural value of treatment and its importance for causal inference. *Annual Review of Statistics and Its Application*.

SÄVJE, F. (2023). Causal inference with misspecified exposure mappings: separating definitions and assumptions. *Biometrika* **111**, 1–15.

SHIN, H., BRAUN, D., IRENE, K., AUDIRAC, M. & ANTONELLI, J. (2023). A spatial interference approach to account for mobility in air pollution studies with multivariate continuous treatments. *arXiv:2305.14194*.

SOFRYGIN, O. & VAN DER LAAN, M. J. (2017). Semi-parametric estimation and inference for the mean outcome of the single time-point intervention in a causally connected population. *Journal of Causal Inference* **5**, 20160003.

SUGIYAMA, M., SUZUKI, T. & KANAMORI, T. (2012). *Density Ratio Estimation in Machine Learning*. Cambridge University Press.

TCHETGEN TCHETGEN, E. J., FULCHER, I. R. & SHPITSER, I. (2021). Auto-G-Computation of causal effects on a network. *Journal of the American Statistical Association* **116**, 833–844.

TCHETGEN TCHETGEN, E. J. & VANDERWEELE, T. J. (2012). On causal inference in the presence of interference. *Statistical Methods in Medical Research* **21**, 55–75.

TEC, M., JOSEY, K., MUDELE, O. & DOMINICI, F. (2024). Causal estimation of exposure shifts with neural networks and an application to inform air quality standards in the US. In *Proceedings of the 30th ACM SIGKDD Conference on Knowledge Discovery and Data Mining*. New York, NY, USA: Association for Computing Machinery.

U.S. CENSUS BUREAU (2024). LEHD origin-destination employment statistics data (2002-2021). <https://lehd.ces.census.gov/data/#lodes>. Accessed: 2024-06-11.

U.S. ENVIRONMENTAL PROTECTION AGENCY (2018). National ambient air quality standards (NAAQS) for nitrogen dioxide. <https://www.federalregister.gov/documents/2018/04/18/2018-07741/review-of-the-primary-national-ambient-air-quality-standards-for-oxides-of-nitrogen>.

U.S. ENVIRONMENTAL PROTECTION AGENCY (2024). Smart location mapping. <https://www.epa.gov/smartgrowth/smart-location-mapping>. Accessed: 2024-06-10.

VAN DER LAAN, M. J. (2014). Causal inference for a population of causally connected units. *Journal of Causal Inference* **2**, 13–74.

VAN DER LAAN, M. J., DUDOIT, S. & KELES, S. (2004). Asymptotic optimality of likelihood-based cross-validation. *Statistical Applications in Genetics and Molecular Biology* **3**, 1–23.

VAN DER LAAN, M. J., POLLEY, E. C. & HUBBARD, A. E. (2007). Super learner. *Statistical Applications in Genetics and Molecular Biology* **6**.

VAN DER LAAN, M. J. & ROBINS, J. M. (2003). *Unified Methods for Censored Longitudinal Data and Causality*. Springer.

VAN DER LAAN, M. J. & ROSE, S. (2011). *Targeted Learning: Causal Inference for Observational and Experimental Data*, vol. 4. Springer.

VAN DER LAAN, M. J. & RUBIN, D. (2006). Targeted maximum likelihood learning. *The International Journal of Biostatistics* **2**.

VAN DER VAART, A. W., DUDOIT, S. & VAN DER LAAN, M. J. (2006). Oracle inequalities for multi-fold cross validation. *Statistics & Decisions* **24**, 351–371.

WALKER, K. & HERMAN, M. (2024). *tidycensus: Load US Census Boundary and Attribute Data as 'tidyverse' and 'sf'-Ready Data Frames*. R package version 1.6.3.

YOUNG, J. G., HERNÁN, M. A. & ROBINS, J. M. (2014). Identification, estimation and approximation of risk under interventions that depend on the natural value of treatment using observational data. *Epidemiologic Methods* **3**, 1–19.

ZHENG, W. & VAN DER LAAN, M. J. (2010). Asymptotic theory for cross-validated targeted maximum likelihood estimation. *bepress*.

ZIGLER, C., LIU, V., MEALLI, F. & FORASTIERE, L. (2023). Bipartite interference and air pollution transport: Estimating health effects of power plant interventions. *arXiv:2012.04831*.

ZIVICH, P. N., HUDGENS, M. G., BROOKHART, M. A., MOODY, J., WEBER, D. J. & AIELLO, A. E. (2022). Targeted maximum likelihood estimation of causal effects with interference: A simulation study. *Statistics in Medicine* **41**, 4554–4577.

Supplementary Materials for
**THE CAUSAL EFFECTS OF MODIFIED TREATMENT POLICIES
 UNDER NETWORK INTERFERENCE**

Salvador V. Balkus

Department of Biostatistics,
 Harvard T.H. Chan School of Public Health
 sbalkus@g.harvard.edu

Scott W. Delaney

Department of Environmental Health,
 Harvard T.H. Chan School of Public Health
 sdelaney@mail.harvard.edu

Nima S. Hejazi

Department of Biostatistics,
 Harvard T.H. Chan School of Public Health
 nhejazi@hsph.harvard.edu

December 12, 2025

These supplementary materials provide proofs of the results presented in the main text, elaborations on some mathematical details, and extra figures and tables for the simulations and data analysis studying the effects of zero-emission vehicle uptake on NO₂ air pollution in California.

S1 Proof preliminaries

As a shorthand, let \mathcal{A} and \mathcal{L} denote the support of A_i and L_i , respectively. Furthermore, let \mathcal{A}_i^s and \mathcal{L}_i^s denote the support of A_i^s and L_i^s (which may differ depending on the unit i as each unit may have different neighbors and network edges). Denote by \mathbf{A}^d the vector $[d(A_i, L_i; \delta)]_{i=1}^n$ so that

$$A_i^{sod} = s_{F_i}(\mathbf{A}^d, \mathbf{L}) \quad (\text{S1})$$

and similarly, $L_i^s = s_{F_i}(\mathbf{L})$. For further brevity, we simplify the exposure summary to either $s(\mathbf{a})$ or $s_{F_i}(\mathbf{a})$ when its dependence on data other than its exposure argument (and set of neighbors, for the latter) is irrelevant to a proof.

We wish to identify the causal estimand $\Psi_n(\mathbf{P}) = \mathbb{E}\left[\frac{1}{n} \sum_{i=1}^n Y(A_i^{sod})\right]$. We begin with a preliminary lemma that will be helpful for identification.

Lemma S1. *Change-of-variables for multidimensional probability densities.*

If $s : \mathbb{R}^n \mapsto \mathbb{R}^k$ with $k \leq n$ is a locally Lipschitz function with Jacobian $J_{\mathbf{a}}s$, \mathbf{A} is a random vector with density function $p_{\mathbf{A}}$, and $A^s = s(\mathbf{A})$, then the density of A^s satisfies

$$\int_{(\mathcal{A})^n} p_{A^s}(s(\mathbf{a})) \sqrt{\det J_{\mathbf{a}}s(\mathbf{a}) J_{\mathbf{a}}s(\mathbf{a})^\top} d\mathbf{a} = \int_{\mathbf{a}^s \in \mathcal{A}^s} \int_{\substack{s(\mathbf{a}) = a^s \\ \mathbf{a} \in (\mathcal{A})^n}} p_{\mathbf{A}}(\mathbf{a}) d\mu(\mathbf{a}) d\mu(a^s), \quad (\text{S2})$$

where μ is the Hausdorff measure, which corresponds to the Lebesgue measure on dense subsets of \mathbb{R}^n . In other words, $p_{A^s}(s(\mathbf{a})) \sqrt{\det J_{\mathbf{a}}s(\mathbf{a}) J_{\mathbf{a}}s(\mathbf{a})^\top}$ is the density of p_A over level sets of s .

Proof. This lemma is a direct application of the *coarea formula*, a generalization of the area formula from multivariable calculus to functions whose Jacobian matrices are not square. The measure-theoretic coarea formula was first proven by Federer (1959, 1969), but Negro (2022) describes its contemporary use for transformations of continuous

random variables. Applying Theorem 3.3 part (ii) with Definition 3.1 of Negro (2022) to the setup given by the above, we have that

$$\begin{aligned} \int_{\substack{a^s \in \mathcal{A}^s \\ \mathbf{a} \in (\mathcal{A})^n}} \int_{s(\mathbf{a})=a^s:} p_{\mathbf{A}}(\mathbf{a}) \partial\mu(\mathbf{a}) \partial\mu(a^s) &= \int_{\substack{a^s \in \mathcal{A}^s \\ \mathbf{a} \in (\mathcal{A})^n}} \int_{s(\mathbf{a})=a^s:} p_{A^s}(s(\mathbf{a})) \partial\mu(\mathbf{a}) \partial\mu(a^s) \\ &= \int_{(\mathcal{A})^n} p_{A^s}(s(\mathbf{a})) \sqrt{\det J_{\mathbf{a}} s(\mathbf{a}) J_{\mathbf{a}} s(\mathbf{a})^\top} \partial\mathbf{a}. \end{aligned}$$

Specifically, the second term follows from the fact that integrating $p_{\mathbf{A}}$ over the level sets of s is equivalent to integrating over p_{A^s} , and the third from Theorem 3.3 of Negro (2022). Interested readers may also consult Lemma 4.4 of Negro (2022), which provides the density of p_{A^s} directly as a function of $p_{\mathbf{A}}(\mathbf{a})$ and $J_{\mathbf{a}} s(\mathbf{a})$ (that is, the reverse of this lemma). \square

Given the assumptions established in the main text, an important remark will permit identification to proceed:

Remark 1. *The piecewise smooth invertibility assumption A3 and the coarea assumption A4 imply that, in an induced MTP, both d^{-1} and s are locally Lipschitz, and therefore $s \circ d^{-1}$ must be locally Lipschitz as well. This implies that Lemma S1 can be applied to $s \circ d^{-1}$.*

S2 Identification

In this section, we use the assumptions defined in the main manuscript to identify the desired causal quantity $\Psi_n(\mathbf{P})$ via a statistical functional ψ_n that is estimable under the observed data structure. First, we can apply iterated expectation to note

$$\begin{aligned} \psi_n &= \mathbb{E}_{\mathbf{P}} \left(\frac{1}{n} \sum_{i=1}^n Y(A_i^{s \circ d}) \right) = \frac{1}{n} \sum_{i=1}^n \mathbb{E}_{Y(A_i^{s \circ d})} (\mathbb{E}_{\mathbf{L}} (Y(A_i^{s \circ d}) \mid \mathbf{L})) && \text{(Iterated expectation)} \\ &= \frac{1}{n} \sum_{i=1}^n \mathbb{E}_{Y(A_i^{s \circ d})} (\mathbb{E}_{A_i^{s \circ d}, \mathbf{L}} (Y(A_i^{s \circ d}) \mid A_i^{s \circ d}, \mathbf{L})) && \text{(No unmeasured confounding)} \\ &= \frac{1}{n} \sum_{i=1}^n \mathbb{E}_Y (\mathbb{E}_{A_i^{s \circ d}, L_i^s} (Y \mid A_i^{s \circ d}, L_i^s)) && \text{(SCM: } Y \text{ only depends on } \mathbf{L} \text{ through } L_i^s) \end{aligned}$$

While technically a statistical quantity in that the final line does not depend on counterfactual distributions of Y , in this problem we only observe \mathbf{A} and \mathbf{L} , not $A_i^{s \circ d}$ and L_i^s . To ensure that this statistical quantity is well-defined, we again apply an iterated expectation over \mathbf{A} and \mathbf{L} , both of which we do observe. Without loss of generality, assume \mathbf{A} and \mathbf{L} are continuous with density $p(\mathbf{a}, \mathbf{l}) = p(\mathbf{a} \mid \mathbf{l})p(\mathbf{l})$. Also, for brevity, let $h_k(\mathbf{a}) = [h_k(a_i)]_{i=1}^n$, and denote the shorthand for the determinant $\Delta f(\mathbf{a}) = \sqrt{\det J_{\mathbf{a}} f(\mathbf{a}) J_{\mathbf{a}} f(\mathbf{a})^\top}$. Then:

$$\begin{aligned} &\frac{1}{n} \sum_{i=1}^n \mathbb{E}_Y (\mathbb{E}_{A_i^{s \circ d}, L_i^s} (Y \mid A_i^{s \circ d}, L_i^s)) \\ &= \frac{1}{n} \sum_{i=1}^n \int_{\substack{l^s \in \mathcal{L}_i^s \\ \mathbf{l} \in (\mathcal{L})^n}} \int_{\substack{s(F_i(\mathbf{l}))=l^s: \\ \mathbf{a} \in (\mathcal{A})^n}} \int_{\substack{a^s \in \mathcal{A}_i^s \\ s(F_i(\mathbf{a}))=a^s:}} \int_{\substack{m((s(F_i \circ d)(\mathbf{a}), s(F_i(\mathbf{l}))p(\mathbf{a}, \mathbf{l}) \partial\mu(\mathbf{a}) \partial\mu(a^s) \partial\mu(\mathbf{l}) \partial\mu(l^s))}} && \text{(Positivity)} \\ &= \frac{1}{n} \sum_{i=1}^n \int_{\substack{l^s \in \mathcal{L}_i^s \\ \mathbf{l} \in (\mathcal{L})^n}} \int_{\substack{s(\mathbf{l})=l^s: \\ (\mathcal{A}_k(l))^n}} \sum_{k=1}^K \int_{\substack{a^s \in \mathcal{A}_i^s \\ (s(F_i \circ h_k)(\mathbf{a}))=a^s: \\ \mathbf{a} \in (\mathcal{A}_k(l))^n}} \int_{\substack{m(s(F_i(\mathbf{a}), s(F_i(\mathbf{l}))p(\mathbf{a}, \mathbf{l}) \partial\mu(\mathbf{a}) \partial\mu(a^s) \partial\mu(\mathbf{l}) \partial\mu(l^s))}} && \text{(Change of level set using Assumption A3)} \\ &= \frac{1}{n} \sum_{i=1}^n \int_{(\mathcal{L})^n} \sum_{k=1}^K \int_{(\mathcal{A}_k(l))^n} m(s(F_i(\mathbf{a}), s(F_i(\mathbf{l}))) \cdot p_{A^s}((s(F_i \circ h_k)(\mathbf{a}) \mid s(F_i(\mathbf{l}))) \Delta(s(F_i \circ h_k)(\mathbf{a}) \partial\mathbf{a} \cdot p_{L^s}(s(\mathbf{l})) \Delta s(\mathbf{l}) \partial\mathbf{l}) && \text{(Lemma S1 and Remark 1)} \end{aligned}$$

The first step follows from positivity because (i) the positivity assumption guarantees $(s_{F_i} \circ d) \in \mathcal{A}^s$, and (ii) m is only a function of summaries, so we only need to integrate over values of the summary with positive probability. In the second step, we note that integrating a function of $(s_{F_i} \circ d)(\mathbf{a})$ over the level set of $s(\mathbf{a}) = a^s$ is equivalent to integrating a function of $s_{F_i}(\mathbf{a})$ over the level set $(s \circ d^{-1})(\mathbf{a}) = a^s$, provided d^{-1} exists; since d is assumed piecewise smooth invertible, we can perform this change of level set on each subset $\mathcal{A}_k \in \mathcal{A}$ as defined in Assumption A3 using the piecewise inverse h_k . In the third step, we apply Lemma S1 to the function $s \circ h_k$ following Remark 1

Next, we multiply and divide by the density of A^s to convert the inner integral to a functional of the observed data and reconstruct the full integral:

$$\begin{aligned} & \sum_{k=1}^K \int_{(\mathcal{A}_k(l))^n} m(s_{F_i}(\mathbf{a}), s_{F_i}(\mathbf{l})) \cdot p_{A^s}((s_{F_i} \circ h_k)(\mathbf{a}) \mid s_{F_i}(\mathbf{l})) \Delta(s_{F_i} \circ h_k)(\mathbf{a}) \partial \mathbf{a} \\ &= \int_{(\mathcal{A})^n} m(s_{F_i}(\mathbf{a}), s_{F_i}(\mathbf{l})) \cdot \sum_{k=1}^K \mathbb{I}(\mathbf{a} \in (\mathcal{A}_k(l))^n) p_{A^s}((s_{F_i} \circ h_k)(\mathbf{a}) \mid s_{F_i}(\mathbf{l})) \Delta(s_{F_i} \circ h_k)(\mathbf{a}) \partial \mathbf{a} \\ &= \int_{(\mathcal{A})^n} m(s_{F_i}(\mathbf{a}), s_{F_i}(\mathbf{l})) \cdot \frac{p_{A^s}((s_{F_i} \circ d^{-1})(\mathbf{a}) \mid s_{F_i}(\mathbf{l})) \Delta(s_{F_i} \circ d^{-1})(\mathbf{a})}{p_{A^s}(s_{F_i}(\mathbf{a}) \mid s_{F_i}(\mathbf{l})) \Delta s_{F_i}(\mathbf{a})} p_{A^s}(s_{F_i}(\mathbf{a}) \mid s_{F_i}(\mathbf{l})) \Delta s_{F_i}(\mathbf{a}) \partial \mathbf{a} \\ &= \int_{(\mathcal{A})^n} m(a^s, l^s) \cdot r(a^s, a^{s \circ d^{-1}}, l^s) \cdot w(\mathbf{a}, \mathbf{l}, i) \cdot p(a^s \mid l^s) \Delta s_{F_i}(\mathbf{a}, \mathbf{l}) \partial \mathbf{a}, \end{aligned}$$

where the final integral notation replaces the summary functions over \mathbf{a} and \mathbf{l} with their shorthand a^s and l^s to emphasize that the nuisances m and r only depend on the values of the summarized variables. Note the use of the notation $p_{A^s}((s_{F_i} \circ d^{-1})(\mathbf{a}) \mid s_{F_i}(\mathbf{l})) \Delta(s_{F_i} \circ d^{-1})(\mathbf{a})$, which by Assumption A3 in the main text will equal the piecewise density $\sum_{k=1}^K \mathbb{I}(\mathbf{a} \in (\mathcal{A}_k)^n) p_{A^s}((s_{F_i} \circ h_k)(\mathbf{a}) \mid s_{F_i}(\mathbf{l})) \Delta(s_{F_i} \circ h_k)(\mathbf{a})$. Assumptions A3 and A4 guarantee that r and w are well-defined almost everywhere. With the inner integral replaced, the statistical estimand becomes

$$\frac{1}{n} \sum_{i=1}^n \mathbb{E}_{\mathbf{P}}(m(A_i^s, L_i^s) \cdot r(A_i^s, A_i^{s \circ d}, L_i^s) \cdot w(\mathbf{A}, \mathbf{L}, i)), \quad (\text{S3})$$

with nuisances denoted, taking $d^{-1}(\mathbf{a}) = [d^{-1}(a_i)]_{i=1}^n$ and $d^{-1}(a_i)$ defined in Assumption A3,

$$\begin{aligned} m(a^s, l^s) &= E_Y(Y \mid A^s = a^s, L^s = l^s) \\ r(a^s, a^{s \circ d^{-1}}, l^s) &= \frac{p_{A^s}(a^{s \circ d^{-1}} \mid l^s)}{p_{A^s}(a^s \mid l^s)} \\ w(\mathbf{a}, \mathbf{l}, i) &= \frac{\Delta(s_{F_i} \circ d^{-1})(\mathbf{a}, \mathbf{l}; \delta)}{\Delta s_{F_i}(\mathbf{a}, \mathbf{l})}. \end{aligned}$$

Because only a single realization of the network \mathbf{F} is observed, identifying the estimand in terms of $m(A_i^s, L_i^s)$, $r(A_i^s, A_i^{s \circ d^{-1}}, L_i^s)$, and $w(\mathbf{A}, \mathbf{L})$ is necessary for ψ_n to be estimable from the data. Note that only the first two nuisance quantities m and r depend on the summaries: w is a known function of only s and d , which are specified by the investigator, and the observed data. Consequently, only the first two nuisances need to be estimated; one can do so non-parametrically by fitting machine learning algorithms based on the summaries A_i^s and L_i^s , rather than needing to estimate the joint density of every individual exposure \mathbf{A} .

S3 Obtaining the efficient influence function

Identification in terms of w and r also permits existing theory to be used for estimation based on the efficient influence function. Recall that a modified treatment policy is a type of stochastic intervention—an intervention that replaces P with some new distribution P^* . The EIF of a stochastic intervention in the network setting of Ogburn et al. (2022) is

$$\frac{1}{n} \sum_{i=1}^n \mathbb{E}(m(A_i^s, L_i^s) \mid \mathbf{L}) + \frac{\bar{p}^*(A_i^s, L_i^s)}{\bar{p}(A_i^s, L_i^s)} (Y - m(A_i^s, L_i^s)) - \psi_n, \quad (\text{S4})$$

where the weighting function for the stochastic intervention is

$$\frac{\bar{p}^*(A_i^s, L_i^s)}{\bar{p}(A_i^s, L_i^s)} = \frac{\frac{1}{n} \sum_{j=1}^n P^*(A_j^s = a_i^s, L_j^s = l_i^s)}{\frac{1}{n} \sum_{j=1}^n P(A_j^s = a_i^s, L_j^s = l_i^s)} \quad (\text{S5})$$

with P^* denoting the probability measure of the replacement distribution. The numerator and denominator are denoted as means because they represent mixture distributions of summaries but are, in practice, estimated together using a single density estimator (Zivich et al., 2022). In our setting, these can be simplified by the law of total probability to marginalize over vectors of neighbors:

$$\begin{aligned} \frac{1}{n} \sum_{j=1}^n P(A_j^s = a_i^s, L_j^s = l_i^s) &= \frac{1}{n} \sum_{j=1}^n P(s_{F_j}(\mathbf{A}, \mathbf{L}) = a_i^s, s_{F_j}(\mathbf{L}) = l_i^s \mid F_j) \\ &= \sum_{j=1}^n P(s_{F_j}(\mathbf{A}, \mathbf{L}) = a_i^s, s_{F_j}(\mathbf{L}) = l_i^s \mid F_j) \frac{\mathbb{I}(F_j = \mathbf{f}_j)}{n} \\ &= \sum_{j=1}^n P(s_{F_j}(\mathbf{A}, \mathbf{L}) = a_i^s, s_{F_j}(\mathbf{L}) = l_i^s \mid F_j) P(F_j) \\ &= P(A^s = a_i^s, L^s = l_i^s) \quad (\text{Law of total probability}) \\ &= P(A^s = a_i^s \mid L^s = l_i^s) P(L^s = l_i^s) \quad (\text{Law of conditional probability}) \end{aligned}$$

where the final probability is the marginal density of A^s and L^s over all possible F_j . The same equality holds for P^* . Hence, we can simply apply the same change-of-variables from our identification result to obtain

$$\begin{aligned} \frac{P^*(A^s = a_i^s, L^s = l_i^s)}{P(A^s = a_i^s, L^s = l_i^s)} &= \frac{P^*(A^s = a_i^s \mid L^s = l_i^s) P(L^s = l_i^s)}{P(A^s = a_i^s \mid L^s = l_i^s) P(L^s = l_i^s)} \\ &= \frac{p_{A^s}(A_i^{sod^{-1}} \mid L_i^s) \Delta(s_{F_i} \circ d^{-1})(\mathbf{A}, \mathbf{L}; \delta)}{p_{A^s}(A_i^s \mid L_i^s) \Delta s_{F_i}(\mathbf{A}, \mathbf{L})} = r(A_i^s, A_i^{sod^{-1}}, L_i^s) w(\mathbf{A}, \mathbf{L}) . \end{aligned}$$

Plugging this into the EIF from Ogburn et al. (2022)—also derived in Sofrygin & van der Laan (2017)—we obtain the EIF for the population intervention effect of an MTP on network \mathbf{F} :

$$\frac{1}{n} \sum_{i=1}^n \left(r(A_i^s, A_i^{sod^{-1}}, L_i^s) w(\mathbf{A}, \mathbf{L})(Y_i - m(A_i^s, L_i^s)) + \mathbb{E}_{\mathbf{P}}(m(A_i^{sod}, L_i^s) \mid \mathbf{L} = \mathbf{l}) \right) - \psi_n . \quad (\text{S6})$$

S4 One-step estimator

Here, we prove that the one-step estimator given by Equation (14) in the main manuscript solves the EIF estimating equation asymptotically and is therefore consistent and semi-parametric efficient under the same estimator regularity conditions as given by Ogburn et al. (2022). As a reminder, for data O_i with a network F admitting a CLT of rate C_n , these regularity conditions are:

A1. *Product rate convergence:* $\|\hat{m} - m\|_2 \|\hat{r} - r\|_2 = o_{\mathbf{P}}(C_n^{-1/2})$.

A2. *Empirical process condition:* $\frac{1}{n} \sum_{i=1}^n \phi_{\hat{P}_n}(O_i) - \phi_{P_n}(O_i) - \mathbb{E}_{\mathbf{P}}(\phi_{\hat{P}_n}(O_i) - \phi_{P_n}(O_i)) = o_{\mathbf{P}}(C_n^{-1/2})$.

Assumption A1 can be satisfied by suitable choices of nuisance estimators. We ensure Assumption A2 using cross-fitting; see Section S6 for further details. Under these assumptions, the following theorem holds:

Theorem S1. *Under assumptions A1 and A2, the simplified one-step estimator is consistent:*

$$\frac{1}{n} \sum_{i=1}^n \phi_{\hat{P}_n}(O_i) \xrightarrow{p} \psi_n \quad (\text{S7})$$

Proof. Solving the EIF in Equation (12) directly for ψ_n yields the quantity

$$\psi_n = \frac{1}{n} \sum_{i=1}^n \hat{r}(A_i^s, A_i^{sod^{-1}}, L_i^s) w(\mathbf{A}, \mathbf{L})(Y_i - \hat{m}(A_i^s, L_i^s)) + \mathbb{E}_{\mathbf{P}}(\hat{m}(h(A_i^s, L_i^s; \delta), L_i^s) \mid \mathbf{L} = \mathbf{l}) . \quad (\text{S8})$$

Distributing the summation linearly, this can be divided into two components, which both converge asymptotically by Theorem 1. The first is the reweighted residual,

$$\begin{aligned} \frac{1}{n} \sum_{i=1}^n \hat{r}(A_i^s, A_i^{s \circ d^{-1}}, L_i^s) w(\mathbf{A}, \mathbf{L})(Y_i - \hat{m}(A_i^s, L_i^s)) \\ \xrightarrow{P} \mathbb{E}_{\mathbf{P}}(r(A_i^s, A_i^{s \circ d^{-1}}, L_i^s) w(\mathbf{A}, \mathbf{L})(Y_i - \hat{m}(A_i^s, L_i^s))) , \end{aligned}$$

which corrects the bias of the plug-in estimate. The second is the plug-in estimate itself,

$$\begin{aligned} \frac{1}{n} \sum_{i=1}^n \mathbb{E}_{\mathbf{A}|\mathbf{L}}(\hat{m}(h(A_i^s, L_i^s; \delta), L_i^s) \mid \mathbf{L} = \mathbf{l}) &\xrightarrow{P} \mathbb{E}_{\mathbf{L}}(\mathbb{E}_{\mathbf{A}|\mathbf{L}}(\hat{m}(h(A_i^s, L_i^s; \delta), L_i^s) \mid \mathbf{L} = \mathbf{l})) \\ &= \mathbb{E}_{\mathbf{L}, \mathbf{A}}(\hat{m}(h(A_i^s, L_i^s; \delta))) , \end{aligned}$$

where the third line follows from the law of total expectation. But, recall that, equivalently, the direct plug-in estimator also converges (assuming \hat{m} is consistent):

$$\frac{1}{n} \sum_{i=1}^n \hat{m}(h(A_i^s, L_i^s; \delta)) \xrightarrow{P} \mathbb{E}_{\mathbf{L}, \mathbf{A}}(\hat{m}(h(A_i^s, L_i^s; \delta), L_i^s)) . \quad (\text{S9})$$

Therefore, by the continuous mapping theorem,

$$\begin{aligned} \hat{\psi}_n^{\text{OS}} &= \frac{1}{n} \sum_{i=1}^n \hat{r}(A_i^s, A_i^{s \circ d^{-1}}, L_i^s) w(\mathbf{A}, \mathbf{L})(Y_i - \hat{m}(A_i^s, L_i^s)) + \frac{1}{n} \sum_{i=1}^n \hat{m}(h(A_i^s, L_i^s; \delta), L_i^s) \\ &\xrightarrow{P} \mathbb{E}_{\mathbf{P}}(\hat{r}(A_i^s, A_i^{s \circ d^{-1}}, L_i^s) w(\mathbf{A}, \mathbf{L})(Y_i - \hat{m}(A_i^s, L_i^s))) + \mathbb{E}_{\mathbf{L}, \mathbf{A}}(\hat{m}(h(A_i^s, L_i^s; \delta))) = \psi_n , \end{aligned}$$

proving that the one-step solves the same estimating equation as Equation (11) asymptotically. \square

S5 Derivation of the variance estimator

In this section we prove that $\hat{\sigma}^2$ as defined in Section 3.5 is a consistent estimator of the variance of $\hat{\psi}_n^{\text{OS}}$, and by extension, the variance of $\hat{\psi}_n^{\text{TMLE}}$. To do this, we establish a few supporting lemmas that hold under the assumptions of the main paper. The first supporting lemma concerns the consistency of the one-step estimator within individual strata of possible $|F_i|$ values; this will constitute an important component of the variance estimator later.

Lemma S2 (Consistency of $\hat{\psi}(|F_i|)$). *A one-step estimator applied to the subset of units with number of friends $|F_i|$ is quarter-root consistent: that is, $\hat{\psi}(|F_i|) - \mathbb{E}(\phi_{\hat{P}_n}(O_i)) = o_{\mathbf{P}}(n^{-1/4})$.*

Proof. In Section 3.2 we assumed that $P(A_i^s) > 0$ for all i . For this assumption to hold true, the number of neighbors of any unit i cannot grow asymptotically slower than that of any other unit j . Formally, this means $|\mathcal{N}(|F_i|)| \propto |\mathcal{N}(|F_j|)|$ for all $i, j \in 1, \dots, n$.

Next, recall that the convergence of the one-step estimator assumes that the maximum degree of any node in the network encoded by \mathbf{F} grows no faster than $n^{1/2}$. More formally, this means $\max_i |F_i| = O(n^{1/2})$. Since $|\mathcal{N}(|F_i|)| \propto |\mathcal{N}(|F_j|)|$, for all i, j , noting that $n/n^{1/2} = n^{1/2}$, it must be true that $|\mathcal{N}(|F_i|)| = O(n^{1/2})$ for all i . Then, noting that under Assumptions A1 and A2, $\hat{\psi}_n^{\text{OS}} - \psi_n = o_{\mathbf{P}}(n^{-1/2})$ for networks of bounded degree, computing the one-step estimator on the subset of nodes $\mathcal{N}(|F_i|)$, which have identical and therefore bounded degree, yields

$$\hat{\psi}_n(|F_i|) - \mathbb{E}(\phi_{\hat{P}_n}(O_i)) = o_{\mathbf{P}}(|\mathcal{N}(|F_i|)|^{-1/2}) = o_{\mathbf{P}}(O(n^{1/2})^{-1/2}) = o_{\mathbf{P}}(n^{-1/4}) . \quad (\text{S10})$$

This completes the proof that the one-step estimator $\hat{\psi}(|F_i|)$ converges to $\mathbb{E}(\phi_{\hat{P}_n}(O_i))$, specifically at rate $o_{\mathbf{P}}(n^{-1/4})$. \square

Next, we prove a lemma demonstrating that the true variance of the centered estimating function is, in fact, the variance that we want to estimate.

Lemma S3 (Bias and variance of estimating function). *The estimating function $\phi_{\hat{P}_n}(O_i) - \hat{\psi}_n(|F_i|)$ is unbiased – that is, $E(\phi_{\hat{P}_n}(O_i) - \hat{\psi}_n(|F_i|)) = 0$ – and, subsequently, its variance is equal to that of the one-step estimator: $Var(\phi_{\hat{P}_n}(O_i) - \hat{\psi}_n(|F_i|)) = Var(\hat{\psi}_n^{OS}) = \sigma^2$*

Proof. First, note that under the assumed SCM (4) in Section 3.2, $\phi_{\hat{P}_n}(O_i)$ and $\phi_{\hat{P}_n}(O_j)$ are identically distributed if $|F_i| = |F_j|$. Consequently,

$$E(\phi_{\hat{P}_n}(O_i) - \hat{\psi}_n(|F_i|)) = E(\phi_{\hat{P}_n}(O_i)) - \frac{1}{\mathcal{N}(|F_i|)} \sum_{j \in \mathcal{N}(|F_i|)} E(\phi_{\hat{P}_n}(O_j)) = E(\phi_{\hat{P}_n}(O_i)) - E(\phi_{\hat{P}_n}(O_j)). \quad (\text{S11})$$

Since $|F_i| = |F_j|$ by definition of $\mathcal{N}(|F_i|)$, $E(\phi_{\hat{P}_n}(O_i)) - E(\phi_{\hat{P}_n}(O_j)) = 0$. Secondly, by mathematical properties of the variance, the variance of our estimating equation can be rewritten as follows:

$$\begin{aligned} \text{Var}\left(\frac{1}{n} \sum_{i=1}^n \phi_{\hat{P}_n}(O_i) - \psi\right) &= \frac{1}{n^2} \sum_{i,j} \mathbb{E}\left((\phi_{\hat{P}_n}(O_i) - E(\phi_{\hat{P}_n}(O_i)))(\phi_{\hat{P}_n}(O_j) - E(\phi_{\hat{P}_n}(O_j)))\right) \\ &= \text{Var}\left(\frac{1}{n} \sum_{i=1}^n (\phi_{\hat{P}_n}(O_i) - E(\phi_{\hat{P}_n}(O_i)))\right) = \sigma^2, \end{aligned}$$

the variance of $\hat{\psi}_n^{OS}$ that we want to estimate, which completes the proof. \square

Theorem S2 (Plug-in variance consistency). *The plug-in variance estimator is consistent:*

$$\hat{\sigma}^2 = \frac{1}{n^2} \sum_{i,j} G(i,j) \varphi_i \varphi_j \xrightarrow{p} \sigma^2, \quad (\text{S12})$$

where $\varphi_i = \phi_{\hat{P}_n}(O_i) - \hat{\psi}_n(|F_i|)$.

Proof. By adding and subtracting to obtain the equality

$$\phi_{\hat{P}_n}(O_i) - \hat{\psi}_n(|F_i|) = \phi_{\hat{P}_n}(O_i) - E(\phi_{\hat{P}_n}(O_i)) + E(\phi_{\hat{P}_n}(O_i)) - \hat{\psi}_n(|F_i|),$$

we can decompose this estimator as follows:

$$\begin{aligned} \hat{\sigma}^2 &= \frac{1}{n^2} \sum_{i,j} G(i,j) \left(\phi_{\hat{P}_n}(O_i) - \hat{\psi}_n(|F_i|) \right) \left(\phi_{\hat{P}_n}(O_j) - \hat{\psi}_n(|F_j|) \right) \\ &= \frac{1}{n^2} \sum_{i,j} G(i,j) \left(\phi_{\hat{P}_n}(O_i) - E(\phi_{\hat{P}_n}(O_i)) \right) \left(\phi_{\hat{P}_n}(O_j) - E(\phi_{\hat{P}_n}(O_j)) \right) \\ &\quad - \frac{2}{n^2} \sum_{i,j} G(i,j) \left(\phi_{\hat{P}_n}(O_i) - E(\phi_{\hat{P}_n}(O_i)) \right) \left(\hat{\psi}_n(|F_j|) - E(\phi_{\hat{P}_n}(O_j)) \right) \\ &\quad + \frac{1}{n^2} \sum_{i,j} G(i,j) \left(\hat{\psi}_n(|F_i|) - E(\phi_{\hat{P}_n}(O_i)) \right) \left(\hat{\psi}_n(|F_j|) - E(\phi_{\hat{P}_n}(O_j)) \right). \end{aligned} \quad (\text{S13})$$

From Ogburn et al. (2022), we know that

$$\frac{1}{n^2} \sum_{i,j} G(i,j) \left(\phi_{\hat{P}_n}(O_i) - E(\phi_{\hat{P}_n}(O_i)) \right) \left(\phi_{\hat{P}_n}(O_j) - E(\phi_{\hat{P}_n}(O_j)) \right) \xrightarrow{p} \sigma^2. \quad (\text{S14})$$

which by Lemma S3 is the desired variance to be estimated. Furthermore, we know that the one-step estimator is $\sqrt{C_n}$ -consistent, and since in Lemma S2 we proved that $\hat{\psi}_n(|F_j|) - E(\phi_{\hat{P}_n}(O_j)) = o_{\mathbb{P}}(n^{-1/4})$, by the continuous mapping theorem,

$$\begin{aligned} &\frac{1}{n^2} \sum_{i,j} G(i,j) \left(\phi_{\hat{P}_n}(O_i) - E(\phi_{\hat{P}_n}(O_i)) \right) \left(\hat{\psi}_n(|F_j|) - E(\phi_{\hat{P}_n}(O_j)) \right) \\ &= \left(\frac{1}{n} \sum_i (\phi_{\hat{P}_n}(O_i) - E(\phi_{\hat{P}_n}(O_i))) \right) \left(\frac{1}{n} \sum_j (\hat{\psi}_n(|F_j|) - E(\phi_{\hat{P}_n}(O_j))) \right) \\ &= o_{\mathbb{P}}(C_n^{-1/2}) \cdot o_{\mathbb{P}}(n^{-1/4}) = o_{\mathbb{P}}(C_n^{-1/2} \cdot n^{-1/4}) \end{aligned} \quad (\text{S15})$$

which is faster than $C_n^{-1/2}$, and also

$$\begin{aligned} & \frac{1}{n^2} \sum_{i,j} G(i,j) (\hat{\psi}_n(|F_i|) - \mathbb{E}(\phi_{\hat{P}_n}(O_i))) (\hat{\psi}_n(|F_j|) - \mathbb{E}(\phi_{\hat{P}_n}(O_j))) \\ &= \left(\frac{1}{n} \sum_i (\hat{\psi}_n(|F_i|) - \mathbb{E}(\phi_{\hat{P}_n}(O_i))) \right) \left(\frac{1}{n} \sum_j (\hat{\psi}_n(|F_j|) - \mathbb{E}(\phi_{\hat{P}_n}(O_j))) \right) \\ &= o_{\mathbb{P}}(n^{-1/4}) \cdot o_{\mathbb{P}}(n^{-1/4}) = o_{\mathbb{P}}(n^{-1/2}), \end{aligned} \quad (\text{S16})$$

implying that the second, third, and fourth terms in Equation (S13) converge to zero. Since the first term converges in probability to σ^2 , we have thereby proven that $\hat{\sigma}^2 \xrightarrow{P} \sigma^2$. \square

S6 Sample-splitting and cross-fitting

Here we establish that the typical as-IID sample splitting and cross-fitting procedure remains valid even in our established network setting. Recall our estimating equation is

$$\frac{1}{n} \sum_{i=1}^n \phi_{\hat{P}_n}(O_i) - \psi_n, \quad (\text{S17})$$

which decomposes into the form

$$\begin{aligned} & \left(\frac{1}{n} \sum_{i=1}^n \phi_{\mathbb{P}_n}(O_i) - \mathbb{E}_{\mathbb{P}}(\phi_{\mathbb{P}_n}(O_i)) \right) + \left(\mathbb{E}_{\mathbb{P}}(\phi_{\hat{P}_n}(O_i) - \phi_{\mathbb{P}_n}(O_i)) \right) \\ &+ \left(\frac{1}{n} \sum_{i=1}^n (\phi_{\hat{P}_n}(O_i) - \phi_{\mathbb{P}_n}(O_i)) - \mathbb{E}_{\mathbb{P}}(\phi_{\hat{P}_n}(O_i) - \phi_{\mathbb{P}_n}(O_i)) \right). \end{aligned}$$

In standard semi-parametric theory, the first term is controlled by the CLT, the second by whether the nuisance estimators converge, and the third by sample-splitting or by invoking empirical process theory. So far, we have used theory from Ogburn et al. (2022)—what remains is only to determine whether the third “empirical process” term can be controlled by cross-fitting.

Essentially, what this requires is that, if we knew the true estimating function $\phi_{\mathbb{P}_n}$, the sample mean constructed as $\frac{1}{n} \sum_i (\phi_{\hat{P}_n}(O_i) - \phi_{\mathbb{P}_n}(O_i))$ would be a **consistent** estimator of the true bias of the estimating function at the correct rate. We establish that this holds in our setting in the following theorem:

Theorem S3 (As-IID Sample Splitting in Network Data). *Let the assumptions of the CLT of Ogburn et al. (2022) hold (Theorem 1 in the main manuscript). Suppose we draw two samples of size n , or “folds,” of indices S_1 and S_2 chosen randomly and independently (i.e., not dependent on the data), and with the nuisance estimators of \hat{P}_n estimated only using $O_i : i \in S_1$. Then,*

$$\frac{1}{n} \sum_{i \in S_2} (\phi_{\hat{P}_n}(O_i) - \phi_{\mathbb{P}_n}(O_i)) - \mathbb{E}_{\mathbb{P}}(\phi_{\hat{P}_n}(O_i) - \phi_{\mathbb{P}_n}(O_i)) = o_{\mathbb{P}}(C_n^{-1/2}). \quad (\text{S18})$$

This means the “empirical process” term is asymptotically negligible.

Proof. Recall that for a statistic to be $o_{\mathbb{P}}(C_n^{-1/2})$ requires two conditions: (1) asymptotic unbiasedness and (2) variance converging to zero at rate $1/C_n$.

We start with (1) asymptotic unbiasedness. Let S denote the set of data over which the set of influence functions is summed. Then,

$$\begin{aligned} \mathbb{E}_{\mathbb{P}} \left(\frac{1}{n} \sum_{i \in S} (\phi_{\hat{P}_n}(O_i) - \phi_{\mathbb{P}_n}(O_i)) \right) &= \frac{1}{n} \sum_{i \in S} \mathbb{E}_{\mathbb{P}}(\phi_{\hat{P}_n}(O_i) - \phi_{\mathbb{P}_n}(O_i) \mid S) \\ &= \sum_{k=0}^{K_{\max}} \mathbb{E}_{\mathbb{P}}(\phi_{\hat{P}_n}(O_i) - \phi_{\mathbb{P}_n}(O_i) \mid S, |F_i| = k) P(|F_i| = k) \\ &= \mathbb{E}_{\mathbb{P}}(\phi_{\hat{P}_n}(O_i) - \phi_{\mathbb{P}_n}(O_i) \mid S) \end{aligned}$$

where the last line follows from the law of conditional expectation, as the summation integrates over all values of K_{\max} , even as $K_{\max} \rightarrow \infty$. Sample splitting becomes necessary when it may be possible that

$$\mathbb{E}_{\mathbb{P}}(\phi_{\hat{P}_n}(O_i) - \phi_{P_n}(O_i) | S) \neq \mathbb{E}_{\mathbb{P}}(\phi_{\hat{P}_n}(O_i) - \phi_{P_n}(O_i))$$

As an example, if $S = S_1$ and our nuisance estimators perfectly interpolated each point in S_1 , then the bias would be $\mathbb{E}_{\mathbb{P}}(\phi_{\hat{P}_n}(O_i) - \phi_{P_n}(O_i) | S_1) = 0$ even though $\mathbb{E}_{\mathbb{P}}(\phi_{\hat{P}_n}(O_i) - \phi_{P_n}(O_i)) \neq 0$ (overfitting). But, if we instead compute the sum over S_2 , chosen randomly such that $S_2 \cap S_1 = \emptyset$, even if the individual data in S_2 are correlated with the data in S_1 , then by the same logic as the above we have

$$\begin{aligned} \mathbb{E}_{\mathbb{P}}\left(\frac{1}{n} \sum_{i \in S_2} (\phi_{\hat{P}_n}(O_i) - \phi_{P_n}(O_i))\right) &= \mathbb{E}_{\mathbb{P}}(\phi_{\hat{P}_n}(O_i) - \phi_{P_n}(O_i) | S_2) \\ &= \mathbb{E}_{\mathbb{P}}(\phi_{\hat{P}_n}(O_i) - \phi_{P_n}(O_i)), \end{aligned}$$

since the choice of indices S_2 is made independently of S_1 and the observed data, and the sample mean is an unbiased estimator even in correlated data.

(2) *Variance converging to zero.* Consequently, whether as-iid sampling-splitting is still valid in the correlated data setting primarily depends on whether its variance converges at the appropriate rate. Under sample splitting, since we just proved that our bias estimator is unbiased,

$$\begin{aligned} \text{Var}\left(\frac{1}{n} \sum_{i \in S_2} \phi_{\hat{P}_n}(O_i) - \phi_{P_n}(O_i)\right) &= E\left(\text{Var}\left(\frac{1}{n} \sum_{i \in S_2} (\phi_{\hat{P}_n}(O_i) - \phi_{P_n}(O_i) | S_2)\right)\right) && \text{(law of total variance)} \\ &= \mathbb{E}\left(\frac{1}{n^2} \sum_{i,j \in S_2} \text{Cov}\left(\phi_{\hat{P}_n}(O_i) - \phi_{P_n}(O_i), \phi_{\hat{P}_n}(O_j) - \phi_{P_n}(O_j) | S_2\right)\right). && \text{(Bienaym\'e's identity)} \end{aligned}$$

By the triangle inequality,

$$\begin{aligned} &\left| \frac{1}{n^2} \sum_{i,j \in S_2} \text{Cov}\left(\phi_{\hat{P}_n}(O_i) - \phi_{P_n}(O_i), \phi_{\hat{P}_n}(O_j) - \phi_{P_n}(O_j) | S_2\right) \right| \\ &\leq \frac{1}{n^2} \sum_{i,j \in S_2} \left| \text{Cov}\left(\phi_{\hat{P}_n}(O_i) - \phi_{P_n}(O_i), \phi_{\hat{P}_n}(O_j) - \phi_{P_n}(O_j) | S_2\right) \right| \\ &= \frac{1}{n^2} \sum_{i,j \in S_2} \left| \text{Corr}(\phi_{\hat{P}_n}(O_i) - \phi_{P_n}(O_i), \phi_{\hat{P}_n}(O_j) - \phi_{P_n}(O_j) | S_2) \right. \\ &\quad \cdot \left. \text{Var}(\phi_{\hat{P}_n}(O_i) - \phi_{P_n}(O_i) | S_2) \cdot \text{Var}(\phi_{\hat{P}_n}(O_j) - \phi_{P_n}(O_j) | S_2) \right|, \end{aligned}$$

so, since the variance of the estimating function under our nuisance estimators must be bounded, we can apply the dominated convergence theorem to conclude that the variance of our bias estimator converges to zero, *provided that* not too many units are correlated.

Having data with a limited number of correlated units is needed to ensure that the above satisfies $\frac{1}{n^2} \sum_{i,j \in S_2} \left| \text{Cov}\left(\phi_{\hat{P}_n}(O_i) - \phi_{P_n}(O_i), \phi_{\hat{P}_n}(O_j) - \phi_{P_n}(O_j) | S_2\right) \right| = o_{\mathbb{P}}(1/C_n)$. Fortunately, since we have assumed $K_{\max} = o(\sqrt{n})$, we have that

$$\begin{aligned} &\frac{1}{n^2} \sum_{i,j \in S_2} \left| \text{Cov}\left(\phi_{\hat{P}_n}(O_i) - \phi_{P_n}(O_i), \phi_{\hat{P}_n}(O_j) - \phi_{P_n}(O_j) | S_2\right) \right| \\ &\leq \frac{nK_{\max}^2}{n^2} \max_{i,j \in S_2} \left| \text{Cov}\left(\phi_{\hat{P}_n}(O_i) - \phi_{P_n}(O_i), \phi_{\hat{P}_n}(O_j) - \phi_{P_n}(O_j) | S_2\right) \right| \\ &= o(K_{\max}^2/n) = o(1/C_n), \end{aligned}$$

because if every unit has K_{\max} neighbors, they will be correlated with K_{\max}^2 units (their neighbors and their neighbors' neighbors), and $n/K_{\max}^2 \leq C_n$ by assumption in the CLT of Ogburn et al. (2022). From this, we conclude that the variance of our empirical process term converges at $o_{\mathbb{P}}(1/C_n)$, the necessary rate.

Finally, since $\frac{1}{n} \sum_{i \in S_2} (\phi_{\hat{P}_n}(O_i) - \phi_{P_n}(O_i))$ is an unbiased estimator of $\mathbb{E}_{\mathbb{P}}(\phi_{\hat{P}_n}(O_i) - \phi_{P_n}(O_i))$ whose variance converges to zero at rate $1/C_n$, we have that the empirical process term is $o_{\mathbb{P}}(C_n^{-1/2})$; hence, as-IID sample splitting still serves its purpose to eliminate the empirical process term in our network setting. The validity of cross-fitting in the correlated data setting for ensuring a fast convergence rate on the empirical process term follows directly from the validity of sample-splitting. \square

S7 Additional Experimental and Data Analysis Results

In this section, we include additional details to supplement the simulation experiments and data analysis conducted in the main manuscript.

S7.1 Further elaboration on the experimental efficiency bound and scaling factor C_n

In the synthetic data experiments, specifically Figure 2, we evaluate performance in terms of the network-TMLE estimator's scaled MSE against a finite-sample efficiency bound. This bound represents the variance of the *ground truth* EIF, computed using the true outcome regression and density ratio functions. For each network structure, we obtain this variance approximately for each possible sample size by drawing a dataset, computing the variance of the ground truth EIF, and then replicating this procedure 10,000 times and averaging the results.

We do this for two reasons. First, as mentioned in the main text, our estimator implicitly conditions on the network structure and estimates a parameter that depends on the sample size, so any efficiency bound should as well. Second, because K_{\max} for each network structure grows roughly at rate $\log(n)$, $C_n^{-1/2} \approx \log(n)/\sqrt{n}$, so the asymptotic efficiency scales with $\log(n)$; this log term ensures even a single very large sample (i.e. $n = 10^6$) cannot possibly reflect an accurate bound to be approached. In light of these, the variance of the asymptotically optimal estimator at each sample size will serve as a reasonable finite-sample efficiency bound, showing us how close to optimal our estimator becomes as n increases.

S7.2 Additional simulation results

In this subsection, we include a few auxiliary simulation results to provide additional insights. First, Figure S1 displays expanded results from the same synthetic data simulation used to create Figure 2 in Section 4.1, this time comparing network-TMLE to a classical “IID” TMLE and a linear regression, neither of which accounts for interference. Breaking out the results separately by network type, we can see that the classical methods incur more bias—and the scaled bias and MSE only increase with sample size. As a consequence, these methods suffer severe under-coverage, which also worsens as the number of samples grows. The gap in performance between network-TMLE and other methods appears largest for the Watts-Strogatz network, which features the greatest degree of connection between units among all of the simulated networks, and therefore the highest amount of interference.

Tables S1 and S2 depict results from additional semi-synthetic data simulations that differed from those of the main text only in the size of the individual exposure effects. In the Table S1 simulation, the mean of the exposure was $\mu_A \approx 8.4$, so most units' exposure resulted in a positive effect. Conversely, in the Table S2 simulation, the exposure mean was $\mu_A \approx 0.4$ —an almost even mix of positive and negative exposures among individual units.

For reference, the main text simulations, which had $\mu_A \approx 3.4$, displayed a simulation set-up where network-TMLE achieved uniformly better performance over both classical TMLE and linear regression, which both ignored interference. These two tables show how varying the magnitude of individual exposure effects can impact differences in performance. On one hand, when most exposures were positive (Table S1), classical methods incurred a much more severe bias and extremely low coverage. Network-TMLE corrects that bias, at the expense of a slight increase in variance compared to classical methods. On the other hand, under a mix of positive and negative exposures, classical methods incurred considerably less bias and much better coverage, but at the expense of a much larger variance than the network-TMLE. This “bias-variance tradeoff” shows how classical methods can fail in different ways when interference is ignored, depending on the treatment effect magnitude.

S7.3 Data analysis summary statistics

Here, we include summary statistics for the dataset used to analyze the effect of zero-emission vehicle uptake on NO_2 air pollution in California. Figure S2 depicts the spatial distribution of the exposure and outcome across the study region of California. Table S3 displays basic summary statistics for the exposure (Change in NO_2 , 2013-2019), outcome (Percentage of ZEVs, 2019), and confounders controlled for in the analysis described in the main manuscript.

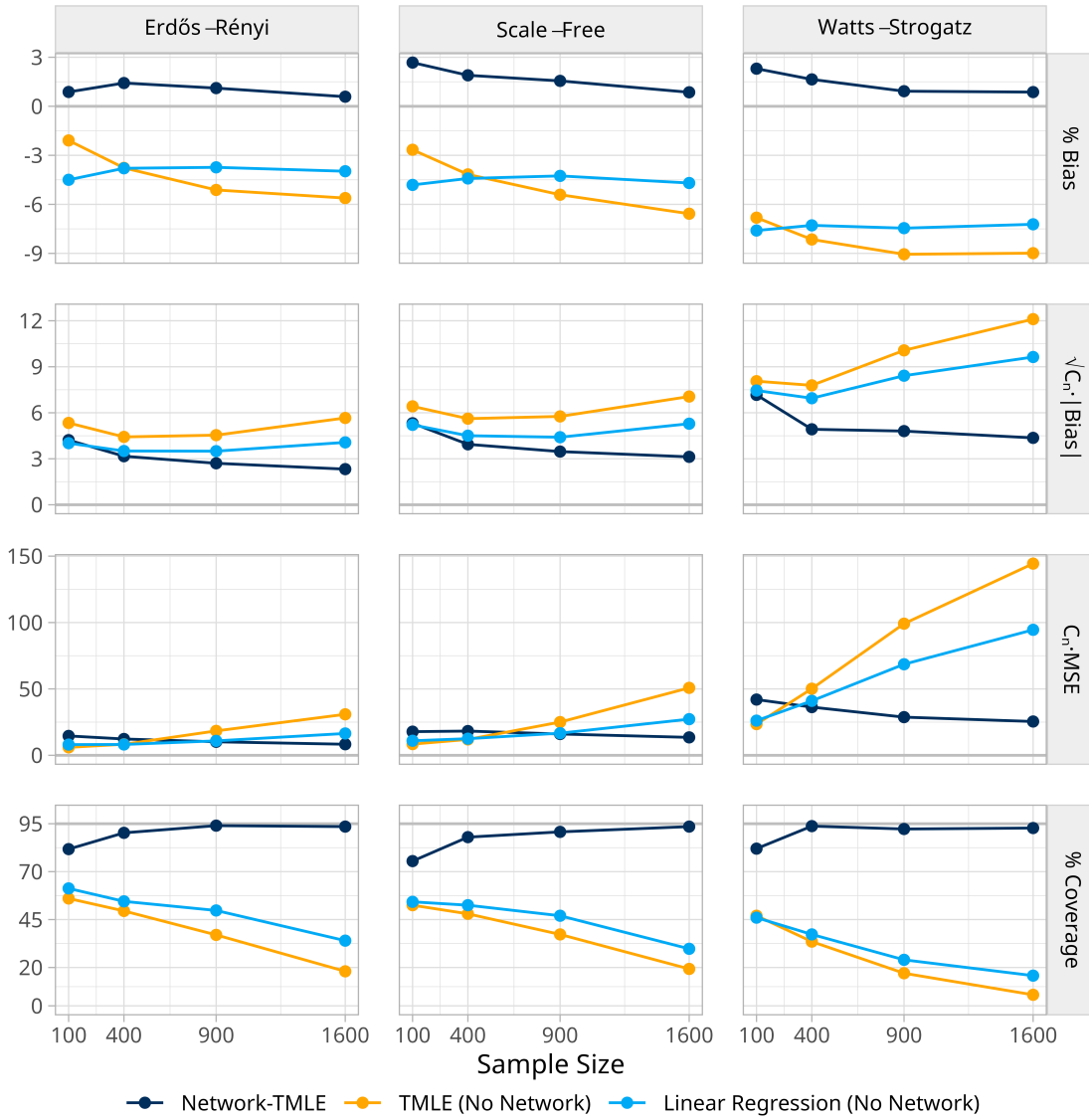


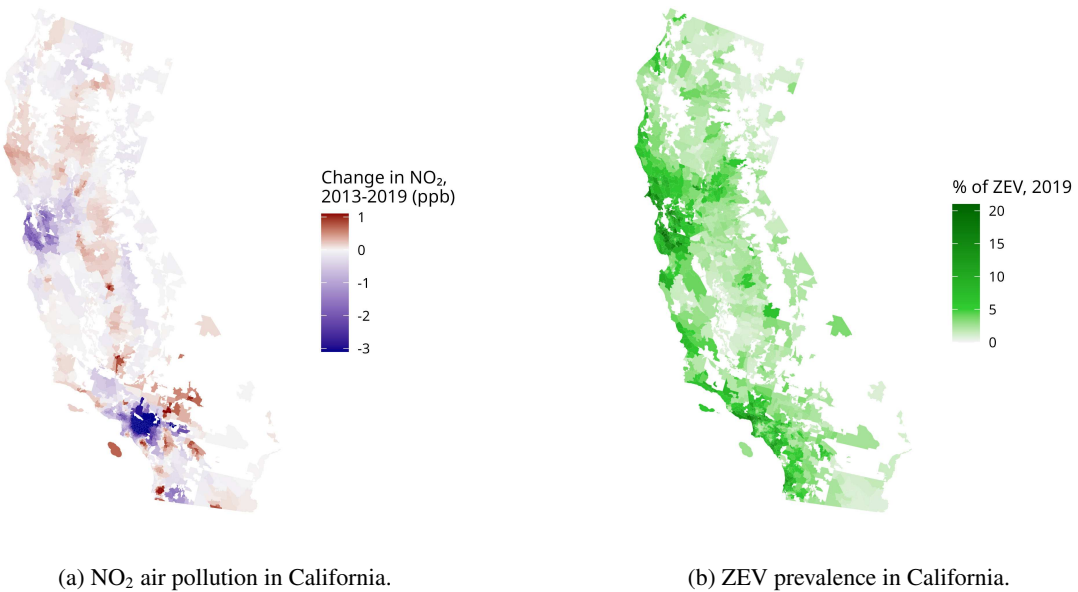
Figure S1: Performance of network-TMLE compared to other common procedures for MTP estimation with various types of network profiles.

Table S1: Semi-synthetic comparison, large exposure effect ($\mu_A \approx 8.4$)

Method	Learner	Bias (%)	Variance	Coverage (%)	CI Width
Network TMLE	Correct GLM	1.54	1.56	94.0	4.88
	Super Learner	2.40	1.58	94.5	4.91
Classical TMLE	Correct GLM	29.10	1.00	32.0	3.92
	Linear Regression	29.53	1.00	31.0	3.92

Table S2: Semi-synthetic comparison, small exposure effect ($\mu_A \approx 0.4$)

Method	Learner	Bias (%)	Variance	Coverage (%)	CI Width
Network TMLE	Correct GLM	0.27	1.56	94.0	4.88
	Super Learner	0.32	1.64	94.5	5.00
Classical TMLE	5.29	5.15	91.8	8.90	
	Linear Regression	5.26	5.16	91.0	8.91

(a) NO₂ air pollution in California.

(b) ZEV prevalence in California.

Figure S2: Spatial distribution of outcome (NO₂) and exposure (ZEV) in the data example.Table S3: Summary statistics of ZEV-NO₂ data, including confounders ($n = 1652$)

Statistic	Mean	Median	25 th pctl.	75 th pctl.
Change in NO ₂ , 2013-2019 (ppb)	-0.6	-0.1	-0.9	0.1
% ZEV (of registered vehicles), 2019	5.4	4.2	2.3	7.6
% ZEV (of registered vehicles), 2013	2.7	2.0	1.1	3.6
Population	23,753	19,505	2,485	38,478
Median income (\$)	76,944	69,156	51,299	95,552
Median home value (\$)	551,847	448,650	277,150	704,850
Median age (years)	40.9	39.2	34.4	46.1
% pop. college educated	32.3	27.7	16.3	46.2
% pop. high school educated	84.7	89.0	78.6	94.4
% pop. white	69.4	73.7	55.7	85.8
% pop. in poverty	10.1	7.5	3.8	14.1
% of homes owner-occupied	59.8	62.6	47.6	74.1
% pop. who take automobile to work	72.8	76.2	69.5	80.2
% pop. who take public transit to work	3.5	1.2	0.0	3.5
% pop. who work from home	8.0	6.0	3.8	9.7
Industrial employment (jobs/acre)	0.6	0.1	0.01	0.5
Road density (per acre)	11.1	6.8	2.4	19.8
Public transit frequency (peak, per hour)	5.4	1.0	0.1	4.9
Walkability index	8.7	7.6	5.1	12.3
Network degree	505.4	594	227.5	742

References

FEDERER, H. (1959). Curvature measures. *Transactions of the American Mathematical Society* **93**, 418–491.

FEDERER, H. (1969). *Geometric measure theory*. Springer.

NEGRO, L. (2022). Sample distribution theory using coarea formula. *Communications in Statistics - Theory and Methods* **53**, 1864–1889.

OGBURN, E. L., SOFRYGIN, O., DÍAZ, I. & VAN DER LAAN, M. J. (2022). Causal inference for social network data. *Journal of the American Statistical Association* , 1–15.

SOFRYGIN, O. & VAN DER LAAN, M. J. (2017). Semi-parametric estimation and inference for the mean outcome of the single time-point intervention in a causally connected population. *Journal of Causal Inference* **5**, 20160003.

ZIVICH, P. N., HUDGENS, M. G., BROOKHART, M. A., MOODY, J., WEBER, D. J. & AIELLO, A. E. (2022). Targeted maximum likelihood estimation of causal effects with interference: A simulation study. *Statistics in Medicine* **41**, 4554–4577.